Russian Chemical Reviews **76** (11) 1023 – 1049 (2007) © 2007 Russian Academy of Sciences and Turpion Ltd

DOI 10.1070/RC2007v076n11ABEH003713

The chemistry of combustion of organophosphorus compounds

O P Korobeinichev, V M Shvartsberg, A G Shmakov

Contents

I.	Introduction	1023
II.	Methods and approaches to investigation of the combustion mechanism of organophosphorus compounds	1024
III.	The mechanism of destruction of organophosphorus compounds in the flame	1026
IV.	Mechanism of promotion and inhibition of the H_2/O_2 flames by addition of organophosphorus compounds	1033
V.	Studies of the mechanism of inhibition and quenching of hydrocarbon flames by organophosphorus additives	1036
VI.	Toxicity and environmental impact of organophosphorus compounds	1046

Abstract. The state of the art of studies on combustion of organophosphorus compounds (OPC) is presented. The chemical processes occurring in flames upon introduction of OPC additives, the mechanisms of OPC transformations and effect on the combustion rate and the structure and propagation limits of hydrogen and hydrocarbon flames are considered. The key results of experimental and theoretical studies and simulation of the combustion chemistry of hydrogen and hydrocarbon mixed and diffusion flames with and without OPC are described. The mechanism of flame promotion and inhibition by OPC is analysed. The prospects of practical applications of phosphorus compounds as flame promotors and suppressants are evaluated. The toxicity and environmental impact of OPC are discussed. The bibliography includes 124 references.

I. Introduction

The chemistry of phosphorus compounds is very extensive and diversified. Phosphorus and its compounds are common in nature ranging from Earth crust minerals to living organisms where phosphorus is vitally important.

The first mention on the investigation into combustion of phosphorus dates back to the 17th century. In 1680, R Boyle [1] burned phosphorus in air and obtained white vapour, which turned into a white powder on cooling. On treating this powder with water, he obtained a liquid with acid properties. Later in has been found that during combustion of phosphorus and its compounds, a large number of phosphorus-containing species are present in the flame. The mechanism of phosphine combustion proposed in 1993 included about 20 phosphorus oxides and phosphorus-containing acids.[2] The existence of numerous phosphorus derivatives in the flames attest to a complex chemical mechanism of transformations of phosphorus and its compounds.

The interest in the combustion chemistry of organophosphorus compounds (OPC) first arose in relation to the problem of destruction of chemical weapons (first of all, nerve agents), which present a serious hazard for both the environment and human life. The combustion of war gases in furnaces formed the basis of an advanced process for the destruction of chemical agent stockpiles. This process was implemented in the USA in the Johnston atoll.[3,4] At that stage, researchers were mainly interested in the mechanism of destruction of complex organophosphorus molecules that simulate chemical agents in a flame.

The term 'destruction' is used to mean the transformation of a compound upon reactions with other flame components or upon pyrolysis rather than its thermal decomposition. The intermediate and final products of OPC destruction in the flame were identified using dimethyl methylphosphonate [DMMP, $CH_3PO(OCH_3)_2$], trimethyl phosphate [TMP, $(CH_3O)_3PO$] and diisopropyl methylphosphonate [DIMP, $CH_3PO(iso\text{-}OC_3H_7)_2$] as models. On the basis of obtained results, reactions of H and OH radicals with OPC molecules were proposed, their rate constants were estimated and a number of kinetic mechanisms of OPC combustion were developed. Subsequently, OPC aroused interest as compounds able to retard (inhibit) combustion.

For many years, halo-substituted, mainly bromo-substituted hydrocarbons (halons) such as CF_3Br have been employed as flame suppressants. However, after these compounds were found to deplete the Earth ozone screen, the production of environmentally hazardous halons ceased in industrially developed countries in conformity with the Montreal convention (1990).[5] Environmentally safe halons like CF_3H and C_2F_5H had low flame suppression efficiency compared to bromine-containing halons; therefore, search for a substitute for halons among other classes of compounds was started. The search led to the OPC family having good prospects as combustion inhibitors.[6–8]

It is noteworthy that OPC do not merely dilute flames (thermophysical flame suppression effect), but rather change the concentration of the most reactive atoms and radicals in the flame, first of all, H, O and OH (chemical suppression of flame by additives), thus having considerable effect on combustion parameters even at low additive concentration (0.03 vol.%).

O P Korobeinichev, V M Shvartsberg, A G Shmakov Institute of Chemical Kinetics and Combustion, Siberian Branch of the Russian Academy of Sciences, ul. Institutskaya 3, 630090 Novosibirsk, Russian Federation. Fax (7-383) 330 73 50, tel. (7-383) 333 28 52, e-mail: korobein@kinetics.nsc.ru (O P Korobeinichev), tel. (7-383) 33 33 46, e-mail: vshvarts@kinetics.nsc.ru (V M Shvartsberg), shmakov@kinetics.nsc.ru (A G Shmakov)

Received 4 April 2007
Uspekhi Khimii **76** (11) 1094 – 1121 (2007); translated by Z P Bobkova

The purpose of this review is to generalise the data on the chemistry and mechanism of OPC transformations in the flames and non-thermal plasma published in the last decades. The review considers in detail the mechanisms of flame promotion, inhibition and suppression by OPC additives. The specific features of inhibition processes for different types of flames are analysed and the dependences of the efficiency of these processes on their conditions (pressure, fuel type, and fuel excess or deficiency) were found. The unique properties of OPC (in particular, physicochemical and toxicological) that distinguish them from other inhibitors were revealed, the effect of OPC on the Earth ozone layer was estimated. On the basis of all the available published data, the prospects for practical applications of phosphorus-containing inhibitors were evaluated.

II. Methods and approaches to investigation of the combustion mechanism of organophosphorus compounds

The chemistry of combustion of organophosphorus compounds has been studied using special experimental and computational methods. Since these processes occur under extreme conditions, many of these methods are actually unique and often poorly known; therefore, below they are described in brief.

1. Experimental methods for investigation of combustion mechanism of organophosphorus compounds

a. Study of the chemical structure of flames by molecular-beam mass spectrometry

The understanding of the essence of chemical kinetic processes taking place in the flames requires knowledge of gas composition in the flames and distribution of combustion product concentrations over the combustion zone. The identification of compounds in the flames and measurement of their concentrations and concentration profiles are usually performed by probe sampling followed by mass spectrometric [9, 10] or optical spectroscopic analysis. Each of the procedures has its advantages; they have repeatedly been used in the research of flames.

Some species found in the flames (atoms, free radicals and ions) are too reactive and unstable to be sampled and analysed by conventional methods; therefore, the sample was introduced into the ionisation chamber of a mass spectrometer as a molecular beam in which molecules did not collide with either one another or the vacuum chamber walls. The profiled probe nozzle and a large pressure differential promote efficient freezing of reactions that occur in the flame, so that quite a robust sample enters the analyser.

Probe molecular beam mass spectrometry (MBMS) is now the only method to detect all species present in the flame (including reactive species), measure their concentrations and spatial distribution, *i.e.*, determine the chemical structure of the flame.[11] However, this method requires additional measures for the separation of substances having similar mass spectra. One of such measures is selective (or so-called soft) ionisation of species in the sample by photoionisation [12, 13] or electron impact.[14, 15] For this purpose, a setup with an advanced ion source with a small energy scatter of electrons (± 0.25 eV) corresponding to thermal scatter was designed at the Institute of Chemical Kinetic and Combustion of the Siberian Branch of the RAS.

Owing to soft ionisation, analysis can be carried out at low ionisation energies close to the ionisation potentials of atoms, radicals and molecules and thus it serves for mitigation (or elimination) of molecular ion fragmentation upon electron impact and, hence, facilitates identification of compounds based on their mass spectra.[14, 15] Table 1 presents ionisation potentials and ionisation voltages (ionisation energies, IE) used to measure the major components of flames with OPC additives: atoms, free radicals and key phosphorus-containing compounds. The ionisation potentials of compounds such as PO, PO_2, HOPO, $HOPO_2$ and $(HO)_3PO$ were determined by measuring the ionisation efficiency curves upon direct sampling of flames with OPC additives. The relative error of measurement of the concentrations of stable compounds in the flame by this method is $< 10\%$, that for radicals is $< 30\% - 50\%$. The perturbing effect of the sampler during flame probing is an important aspect influencing correct interpretation of the experimental results. In recent years, a number of experimental and computational studies dealing with the flame perturbation by the probe were published (see, for example, Refs 16, 17). The results obtained in these studies substantiate the efficiency of using the experimental temperature profile for simulation of the concentration profiles of compounds in the flame.

Table 1. Ionisation potentials and ionisation electron energies for major components of the flame with OPC additives.

Compound or species	m/z	Ionisation potential /eV	Ionisation electron energy in the experiment /eV
PO	47	8.3 ± 0.3	12.8
PO_2	63	11.0 ± 0.5	12.8
HOPO	64	10.7 ± 0.3	12.8
$HOPO_2$	80	12.4 ± 0.2	14.5
$(HO)_3PO$	98	11.5 ± 0.5	17.5
$(CH_3O)_2(CH_3)PO$	124	9.9 ± 0.5	20.0
$(CH_3O)_3PO$	140	9.9 ± 0.5	20.0
H	1	13.3 ± 0.5	16.2
O	16	13.6 ± 0.2	16.2
OH	17	13.2 ± 0.2	16.2

b. Measurement of flame temperature using thermocouples

The temperature distribution across the combustion zone is usually measured by microthermocouples [Pt/(Pt + 10% Rh) and so on] with different diameters. For preventing catalytic processes, the thermocouple surface is coated by SiO_2 or ceramics.[18] The emission corrections were estimated by the Kaskan formula [19] or excluded by using compensation measurements.[20] The agreement between the temperature and concentration profiles across the zone was attained by shifting the concentration profiles with respect to the temperature profile.[21] The error of temperature measurement usually did not exceed ± 30 K.

c. Methods of measurement of normal flame propagation speed

Several methods exist for measuring of the normal propagation speed of the flame front in laminar pre-mixed gas mixtures. One method is based on the use of the Mache – Hebra burner,[22] which provides the contour of the visible image of the flame as a regular cone. The accuracy of measurement of the flame speed by this method is $\pm 5\%$. This method for flame propagation speed measurement is very convenient due to its simplicity and availability but is considered to be least accurate.

The technique of zero heat flux to the burner, which has found wide use in recent years, is more accurate.[23, 24] This method makes use of a flat burner consisting of a copper disc with evenly distributed holes and the side surface cooled by tap water. The radial temperature distribution over the burner surface is measured by insertion of thermocouples into its holes at different distances from the burner centre. When temperature is evenly distributed over the burner disc surface, a heat flux from the flame to the burner is absent, the flame existing

under nearly adiabatic conditions. This means that the flow rate of the combustible mixture is equal to the free distribution speed of the flame.

The method of measurement of the normal speed of flame propagation using a constant volume bomb also deserves attention.[25] This measurement requires a special high-pressure chamber, as ignition of the combustible mixture results in substantial pressure rise in a closed vessel.

d. Methods of determination of the minimum quenching concentrations of flame suppressants

The minimum quenching concentration (MQC) is a concentration of a substance in the flame such that the flame is quenched when this concentration has been attained. This is an important characteristics for evaluating the prospects of using a particular compound as a flame suppressant. A standard method for determining the MQCs of flame suppressants [26, 27] is the cup burner method. It consists of suppression of the diffusion methane – air or n-heptane – air flame by introducing flame suppressant vapour into the air stream.[27] Poorly volatile (liquid) compounds are injected into the air stream by means of a nebulizer. Air is heated to enhance evaporation rate of the aerosol of the liquid compound. Yet another, alternative method for determination of MQC is the 'cylinder' method described by Baratov *et al.*[28, 29] Whereas the cup burner method implements a scenario of extinguishing a local ignition source by an air stream with admixed flame suppressants, the 'cylinder' method is based on a fire extinguishing scenario in an indoor area.

One more method, the fire chamber method, is used to determine the MQC of flame suppressants under nearly natural conditions. These measurements require a large amount of flame suppressant; therefore, this method cannot be used for screening.

A special setup was designed to study the quenching efficiency of a turbulent † flame upon short-term supply of a flame suppressant.[30] Using this setup, the dependence of MQC on the supply time of the flame suppressant and the fuel volumetric flow rate was studied. For the study of turbulent flame quenching by poorly volatile liquid OPC, a setup similar to that described previously [30] was manufactured.[31] Both simulate aircraft engine fire extinguishing. Liquid flame suppressants were supplied by a highly dispersed aerosol generator (particle size < 1 μm) of an original design.[31]

2. Numerical simulation and quantum chemical calculations

a. Simulation software

The chemistry of OPC combustion is often studied by numerical simulation, which allows one to calculate the propagation speed and the chemical and thermal structures of multicomponent laminar and diffusion flames. Model calculations use thermochemical and transport characteristics of flame components, detailed chemical mechanism of the combustion process as a set of elementary steps with indicated rate constants for each step. These calculations were carried out using PREMIX and CHEMKIN softwares.[32, 33] The PREMIX programme calculates (for a unidimensional case) the flame propagation speed and the temperature and component concentration profiles in a freely propagating flame or a flame stabilised on a flat burner. The CHEMKIN-II programme and later versions CHEMKIN-III and CHEMKIN-IV softwares choose the required thermochemical, kinetic and transport characteristics of flame components from the databases included in the program package. All calculations are based on solution of the energy conservation equation with allowance for diffusion.

† A turbulent flame site above a tank with liquid fuel is most difficult for extinguishing, expecially if the tank is located behind a wedge-like barrier.

One can also use the HCT programme (Hydrodynamics, Chemistry and Transport) [34] developed at the Lawrence Livermore National Laboratory (USA) and the OPPDIF programme,[35] which is a part of the CHEMKIN package. The latter programme was used to calculate the temperature and component concentration profiles, the radial and axial constituents of the flow velocities along the burner axis in the diffusion flame stabilised at the counterflow of the fuel and the oxidant (the Potter burner [36, 37]).

b. Kinetic mechanisms

Although the kinetic models of hydrogen and hydrocarbon combustion bear only an indirect relation to the OPC combustion chemistry, the results of simulation of the structure or propagation speed of OPC-doped flames still depend appreciably on the selected mechanism for hydrogen and hydrocarbons. In this connection, we considered it necessary to present brief information on the most often encountered mechanisms of combustion of these compounds.

The rate constants for reactions that describe the hydrogen combustion process have been reported.[38–40]. The H_2 combustion was studied in detail by Dixon-Lewis *et al.*,[41] Tsang and Hampson [42] and Yetter *et al.*[43] A kinetic scheme of hydrogen combustion that includes 40 most important elementary steps involving 8 species has been described.[44] Although this process has been well studied, a large number of models that differ from one another in both the set of reactions and the rate constants for these reactions can be found in the literature. The latest model of hydrogen oxidation under atmospheric pressure was developed in 2004.[45]

Hydrocarbon flames can be simulated using the GRI-Mech mechanism [46] describing the combustion of natural gas in the presence of nitrogen. A version of this mechanism, namely, GRI-Mech 3.0 comprises 325 reactions involving 53 components (including argon). One more, Konnov's mechanism [47] includes 1207 reactions involving 127 components. This is used to describe the combustion of hydrocarbons ($\leqslant C_3$) and their derivatives. The last-mentioned mechanism was successfully used to calculate the speed of free propagation of propane – air flames.[47] The results are in good agreement with experimental results.[48, 49] The kinetic mechanism of propane combustion proposed by Conaire *et al.*[50] and upgraded by Curran *et al.*[51] was used to describe the structure of propane – oxygen flames with OPC additives stabilised on a flat burner [52] and to calculate the propagation speed of propane – air flames.[53] The mechanism includes 469 steps which involve 77 components.

c. Quantum chemical calculations

The thermochemistry of phosphorus-containing compounds has little been studied until recently. Only recently, was this field of OPC chemistry developed owing to quantum chemical calculations,[54–56] which became much more precise. This is especially important, as phosphorus oxides are unavailable as commercial chemicals due to their low stability. Table 2 presents the formation enthaplies of PO, PO_2, PO_3, HOPO, $HOPO_2$, $(HO)_2PO$, HPO, HPO_2, P_2O_3, P_2O_4 and P_2O_5(gas). Not only thermochemical parameters of OPC (enthalpy, entropy), but also the rate constants for some key reactions of phosphorus-containing species with atoms (H, O, C, N) and radicals were calculated.[52, 53]

As shown below, these calculations identify more precisely the previously developed kinetic mechanisms and provide better agreement between the experimental data and the results of simulation of the flame propagation speed and chemical structure.

A considerable contribution to the development of OPC combustion mechanism and the kinetic model of the process was made by theoretical works carried out at the Lawrence

Table 2. Formation enthalpies (ΔH_f° /kJ mol^{-1}) of phosphorus-containing compounds calculated by various methods.

Compound	BAC-MP4 (Ref. 54)	CBS (Ref. 56)	BAC-G2 (Ref. 52)	G3X2 (Ref. 55)
PO	−12.6	−33	−37	−38
PO_2	−283	−294.9	−298	−291
PO_3	−430	−450	−450	
HOPO	−452	−470	−468	−470
$HOPO_2$	−690	−717	−719	−713
$(HO)_2PO$	−647		−661	−664
HPO	−75	−95	−96	
HPO_2	−406		−425	
P_2O_3	−616		−658	
P_2O_4	−855		−908	
P_2O_5	−1072		−1135	

Livermore National Laboratory (USA) . The OPC combustion model proposed at this laboratory was based on quantum chemical calculations of the thermochemical properties of phosphorus-containing molecules and transition states and reaction rate constants. This approach is more substantiated from the kinetic standpoint as compared with mere variation of the rate constants, as was done in the early investigations. The thermochemical data (enthalpy, entropy and heat capacity) were calculated for 25 compounds of pentavalent phosphorus in which the phosphorus atom is bound to hydrogen, carbon, nitrogen or sulfur atoms.

3. Integrated approach to elucidation of the combustion mechanism of organophosphorus compounds

An efficient approach to investigation of the OPC combustion chemistry is a comparison of experimental and simulated data. The larger the number of combustion characteristics being compared (propagation speed and chemical structure of the flame, propagation limits, minimum quenching concentrations and so on) the more thorough the verification of the proposed kinetic model and the more reliable the model. A problem of many (almost all) kinetic mechanisms is that they have been validated against a limited number of data.

It is noteworthy that the combustion mechanism depends on the stoichiometric composition of the fuel mixture. In the fuel-rich flames, the processes are complicated due to the formation of heavy hydrocarbons, soot precursors. These flames are most often difficult to study, and general hydrocarbon combustion models often poorly predict the characteristics of these flames.

The most thorough verification for any mechanism is a comparison of the calculated and measured flame structures, first of all, a comparison of the concentration profiles of atoms, radicals and other unstable species. This approach was used to study the chemistry of OPC combustion and especially to study the mechanism of inhibition of hydrocarbon flames by TMP.

III. The mechanism of destruction of organophosphorus compounds in the flame

The first soft ionisation MBMS study [57] devoted to the OPC transformations in the flames (1994) reported the mass spectra of samples taken from the flame and the intensity profiles for ion peaks with m/z corresponding to the initial compounds and intermediate and final products of TMP and tributyl phosphate (TBP) combustion in a hydrogen – oxygen flame at a pressure of 80 Torr. When measuring the TMP and TBP concentration in the flame, it was shown that OPC in a low-pressure hydrogen – oxygen flame are consumed faster than the major flame components (H_2 and O_2). Systematic research into the mechanism of destruction of DMMP, TMP, DIMP, and some other OPC was carried out in the subsequent studies.

1. Mechanism of destruction of dimethyl methylphosphonate

In a study of the structure of a hydrogen – oxygen flame doped with DMMP at 47 and 76 Torr, key intermediates of DMMP destruction with masses of 110 and 94 were detected and identified as methyl methylphosphonate and methylphosphonic acid, respectively. The final phosphorus-containing products of DMMP combustion with m/z 47, 63, 64 and 80 were identified as (PO), (PO_2), (HOPO) and ($HOPO_2$).[14, 58, 59]

a. Intensity profiles of the mass peaks of the starting dimethyl methylphosphonate and the intermediate and final products of its destruction

In order to analyse the possible intermediates of DMMP destruction, mass spectra of samples taken from the H_2/O_2/Ar flame (P = 47 Torr) doped with 0.2 vol.% DMMP were recorded. The flame samples were taken at distances of $\leqslant$4 mm from the burner (within the DMMP destruction zone in the flame).[14] The ion peaks with m/z 79, 80, 81, 93, 94, 95, 96, 98, 109, 110 were found in the mass spectra of the samples. The contributions of the fragment ions resulting from ionisation of the DMMP molecule to these peaks were eliminated using a mass spectrum of DMMP recorded in an argon flow. Note that the mass spectrum of DMMP recorded in this way does not contain ion peaks with m/z 110 or 80.

Figure 1 shows the intensity profiles of the peaks of DMMP with m/z 124 and ions with m/z 110, 94 and 80 (with subtracting the contributions of fragment ion peaks) depending on the distance (l) from the burner surface to the probe at P = 43 Torr and IE = 12.1 eV. The intensity profiles of ion peaks with m/z 110, 94 and 80 pass through maxima; the intensity maxima of the peaks with m/z 110 and 80 are located at a 1.5 mm distance from the burner, while that for the peak with m/z 94 is at a 2.5 mm distance from the burner. Figure 2 shows the intensity profiles of the peaks of DMMP and ions with m/z 95, 96, 98 and 110 (with subtracting the small contributions of fragment ion peaks) depending on the distance l for P = 47 Torr and IE = 20 eV. The presence of maxima in the intensity curves for ion peaks with m/z 80, 94, 95, 96, 98 and 110 indicates that these peaks may correspond to intermediates.

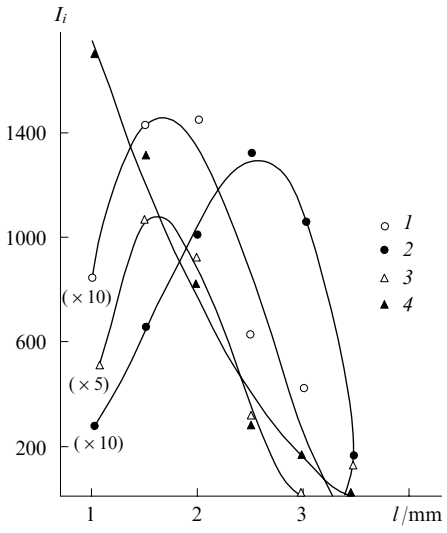


Figure 1. Intensity profiles of ion peaks with m/z 80 (curve *1*), 94 (*2*), 110 (*3*) and 124 (*4*) in the H_2/O_2/Ar flame with 0.2 vol.% DMMP at P = 43 Torr and IE = 12.1 eV.[14]

There are two intermediates with the mass 110: dimethyl phosphonate [$HPO(OCH_3)_2$] and methyl methylphosphonate [$HOPO(OCH_3)(CH_3)$]. Under electron impact, both com-

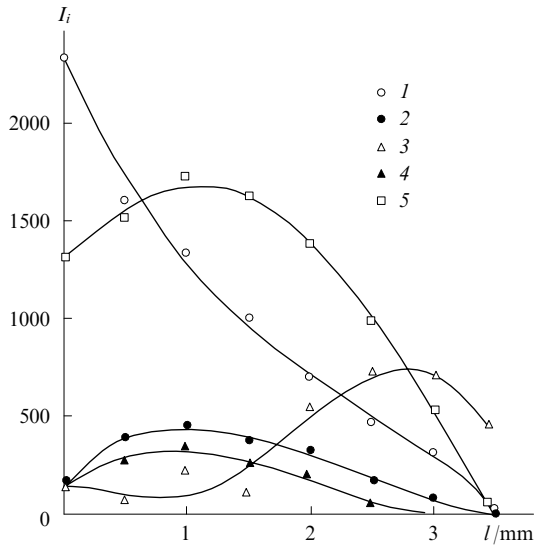


Figure 2. Intensity profiles of the peaks of initial DMMP (curve *1*) and ions with m/z 110 (curve *2*), 98 (*3*), 96 (*4*) and 95 (*5*) in the $H_2/O_2/Ar$ flame with 0.2 vol.% DMMP at $P = 47$ Torr and IE = 20 eV.[14]

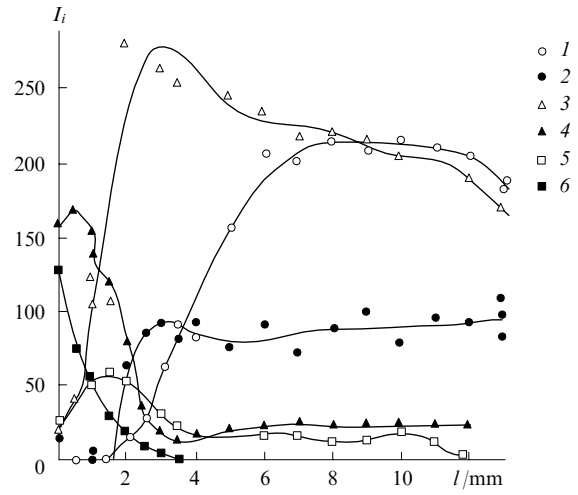


Figure 3. Intensity profiles of ion peaks with m/z 47 (PO, curve *1*), 63 (PO_2, curve *2*), 64 (HOPO, curve *3*), 80 (curve *4*), 98 [$(HO)_3PO$, curve *5*] and 124 (DMMP, curve *6*) in the $H_2/O_2/Ar$ flame with 0.2 vol.% DMMP at $P = 47$ Torr and IE = 13.4 eV.[14]

pounds give species with masses of 95 and 80;[60] therefore, ion peaks with m/z 95 and 80 correspond to intermediate fragment compounds (presumably, decomposition products of methyl methylphosphonate [14]). The peak with m/z 96 corresponds to methylphosphonic acid [$(HO)_2PO(CH_3)$]. The intensity of the ion peak with m/z 81 is approximately twice as high as the intensity of the m/z 98 peak, and the behaviour of the intensity curve of the m/z 81 peak fully reproduces that for the ion peak with m/z 98. The ion with mass 81 may thus be a fragment ion of a compound with mass 98 (this compound was identified as orthophosphoric acid). The ion with mass 94 was identified as the $PO_2(OCH_3)$ molecular ion. The ion peaks with m/z 79, 93 and 109 correspond to the fragment ions formed upon bombardment of DMMP with electrons. The mass spectra of samples taken from flames were also found to contain peaks corresponding to species with m/z 28 (CO), 44 (CO_2), 47 (PO), 63 (PO_2) and 64 (HOPO).

The intensity profiles of ion peaks with m/z 47, 63, 64, 80 and 98 recorded for flames doped by 0.2 vol.% DMMP at $P = 47$ Torr are presented in Fig. 3. The ion peak with mass 80 has a maximum at a ~ 1 mm distance from the burner surface. It was found that different substances are responsible for contributions to the ion peak with m/z 80 at different distances from the burner surface. Thus analysis of the curve of DMMP ionisation efficiency has shown that the peak with m/z 80 recorded in the flame at a 1 mm distance from the burner surface has the appearance potential $AP = 11.5 \pm 0.3$ eV, while the ion peak with the same mass detected at a distance of 7–10 mm has $AP = 13.5 \pm 0.5$ eV. Analysis of the mass spectra [60] of the presumed intermediate product, *viz.*, methyl methylphosphonate (mass 110), indicates that it is fragmented upon electron impact to give an ion with mass 80. Thus, at distances of up to 3 mm (where the ion with m/z 110 was detected as an intermediate), the major contribution to the intensity of the peak with m/z 80 is due to the methyl methylphosphonate fragment ion. At distances $l > 3$–4 mm from the burner surface (*i.e.*, in the final products of DMMP destruction), the molecular ion of $HOPO_2$ with the same mass appears in the flame.

Analysis of the concentration profiles of intermediates recorded in the $H_2/O_2/Ar$ flame doped with 0.2 vol.% DMMP suggests the following sequence of DMMP transformations in the flames (possible compounds corresponding to these masses are given in brackets):

$$124\ (DMMP) \longrightarrow 110, 95, 80\ [HOPO(CH_3)(OCH_3)] \longrightarrow$$
$$\longrightarrow 96\ [(HO)_2PO(CH_3)], 94\ [PO_2(OCH_3)] \longrightarrow$$
$$\longrightarrow 98\ [(HO)_3PO] \longrightarrow 80\ (HOPO_2), 64\ (HOPO), 63\ (PO_2), 47\ (PO).$$

For interpreting the obtained experimental results, the possible fragmentation routes of DMMP (subsequently, also TMP) in the $H_2/O_2/Ar$ flame were analysed. The following types of reactions were considered:

(i) unimolecular decomposition and four-centre reactions;

(ii) bimolecular elimination of H, CH_3 and OCH_3 from the DMMP molecule by H, O and OH radicals and the substitution of alkyl and alkoxyl groups;

(iii) bi- and trimolecular recombination reactions.

The enthalpies of the reactions were calculated using the enthalpies of formation of some OPC estimated by Melius.‡ On the basis of these data, a detailed kinetic mechanism of DMMP destruction in the flame was proposed.[58] Subsequently, this mechanism was upgraded (reactions from the mechanism proposed by Twarowski [61–63] were also included).

b. The Twarowski mechanism

An important step towards the understanding of the mechanism of OPC effect on flames was made after they were found to be applicable for increasing the efficiency of a ramjet fueled by hydrogen. It was found that combustion of hydrogen at high altitudes and, hence, at low pressures gives H and OH radicals in super equilibrium concentrations in the combustion chamber. These radicals have no time to recombine in the combustion chamber and are carried away to atmosphere, resulting in a loss in the engine power. For increasing the completeness of combustion, it was proposed to add phosphine to the fuel; this additive ensured an additional kinetic channel of recombination of H and OH radicals to give water. Twarowski [2, 61–63] carried out a series of studies dealing with the effect of phosphine additive on the H and OH radical recombination rate in the flame. On measuring the variation of the concentrations of OH radicals formed upon combustion of a diffusion hydrogen–oxygen flame in the presence of phosphine vapour by laser-induced fluorescence, Twarowski [2]

‡ Private communication (1996, the Lawrence Livermore National Laboratory, USA).

assumed that recombination of OH radicals is catalysed by phosphorus oxides and phosphorus-containing acids: PO, PO_2, HOPO and $HOPO_2$. He proposed a mechanism for catalytic recombination of H and OH radicals with participation of these phosphorus compounds; in more recent works,[61–63] he supplemented this mechanism by new reactions with modified rate constants.

c. Analysis of the destruction mechanism

In a study [14] devoted to determination of the general mechanism of OPC transformations in the flame, it was shown that destruction of OPC takes place through replacement of CH_3 and CH_3O groups by H and OH radicals. The full spectrum of the final phosphorus-containing products of OPC combustion was also identified. The obtained results served as the prerequisite for the design of other models for OPC destruction in flames on the basis of detailed kinetics and calculations of structures and propagation velocities of OPC-doped flames.

An essential contribution to the study of chemistry and mechanism of OPC destruction in flames was made by Werner and Cool,[13] who investigated the chemical structure of rich hydrogen–oxygen flames doped with 0.1 vol.% DMMP.§ On the basis of the obtained results, they developed a kinetic model for DMMP destruction in the flames. Using soft UV ionisation MBMS, they identified a number of intermediates of DMMP destruction in the flame such as $(CH_3)PO_2$ (78), $(CH_3O)PO$ (78), $(CH_3)(CH_3O)(OCH_2)PO$ (123), $(HO)_2PO(CH_3)$ (94) and $HOPO(CH_3)(OCH_3)$ (110) (the values in parentheses are the molecular masses of the products). It was shown experimentally [13] that the destruction occurs upon the reaction of DMMP molecule with H and OH radicals (mainly, with replacement of alkyl and alkoxyl substituents by OH groups).

Werner and Cool [13] also calculated the rate constant for the thermal decomposition of DMMP. According to their data, the activation energy of the reaction of DMMP with OH equals 365 kJ mol^{-1}, indicating a negligibly low contribution of DMMP pyrolysis during combustion. On the basis of their own experimental results [13] and earlier data [14] and resorting to quantum chemical calculation data obtained by Melius, Werner and Cool [13] proposed the first detailed mechanism of DMMP destruction in the flame. Using this mechanism, the flame structure was simulated and the results were compared with the experiment. Unfortunately, the researchers did not measure the concentrations of final and intermediate phosphorus-containing combustion products (including stable ones); therefore, the concentration intensity profiles across the combustion zone were equated (in the maximum) to the maximum concentrations of these compounds found by simulation. This somewhat decreases the significance of the work,[13] as the lack of quantitative experimental results did not allow them to verify whether the model can correctly predict the distribution of combustion product concentrations across the flame zone.

The knowledge of the presence of the above-listed compounds in DMMP-doped flames was used by some researchers to design their own models for DMMP destruction in the flames and to calculate the chemical structure and the free propagation speed of a flame with DMMP additive (see, for example, Refs 64 and 65).

Quantitative measurement of the concentrations of combustion products was the next step towards the understanding of the OPC combustion chemistry.[66] Thus the proposed mechanisms of OPC destruction were verified by comparing the simulation data with experimental results on the flame structure, and this allowed the researchers to perfect the mechanisms. Since direct calibration of a MBMS unit used to study the OPC transformations in the flame with respect to PO, PO_2, HOPO or $HOPO_2$ is impossible due to their instability and, hence, the lack of these compounds, their calibration coefficients were determined from the phosphorus material balance in the flame. Metaphosphoric acid $HOPO_2$, which exists as the crystals $(P_2O_5)_x(H_2O)_y$, where $x:y \approx 1:1$, can be considered an exception. However, the extremely low saturated vapour pressure of this acid precludes direct calibration of the unit with respect to this compound.

The calibration factors of phosphorus oxides and phosphorus-containing acids were determined by measuring the intensities of peaks of ions with m/z 40 (Ar), 47 (PO), 63 (PO_2), 64 (HOPO) and 80 ($HOPO_2$), *i.e.*, the final products of DMMP and TMP combustion in hydrogen–oxygen flames with different composition. The introduction of knowingly larger number of equations than variables into the set of phosphorus balance equations (the set of equations was overdetermined) owing to the large number of peak intensity measurements in the flames with different composition increased the calculation accuracy. The calculated calibration coefficients were used to determine the concentration profiles for PO, PO_2, HOPO and $HOPO_2$ in a hydrogen–oxygen flame with OPC additive.

The structure simulation of burner-stabilised flames used, as the input data, the temperature profiles measured by a thermocouple with a junction located near the probe orifice. Simulation of the structure of the $H_2/O_2/Ar$ flames in the presence of DMMP [58] in terms of the Twarowski mechanism [2] demonstrated that with reaction rate constants proposed by Twarowski, the model predicts incorrectly the concentrations of these components. Analysis of the sensitivity of the rate constants of reactions comprised in the Twarowski kinetic mechanism (Table 3) to the concentrations of phosphorus oxides and phosphorus-containing acids showed that agreement between the simulation and measurement results can be attained by increasing the rate constants for trimolecular reactions 3, 5, 10 and 13 and simultaneously decreasing the rate constants for bimolecular reactions 2, 4, 7, 8, 9, 11, 12 and 14. Such changes in the rate constants resulted in an increase in the calculated $HOPO_2$ concentration and a decrease in the PO concentration. As a result, the concentration ratio $[HOPO]/[PO_2]$ approached the experimental value.

Previously, incorporation of a number of primary steps giving rise to $HOPO(CH_3)(OCH_3)$ (m/z 110), $HOPO(OCH_3)_2$ (126), $HOP(CH_3)(OCH_3)_2$ (125) and $PO(CH_3)(OCH_3)(OCH_2)$ (123) into the DMMP destruction mechanism has been proposed.[13,14] In the study considered,[58] reactions involving $HOP(CH_3)(OCH_3)_2$ (m/z 125) were not included in the final DMMP destruction model, as sensitivity analysis of the consumption rate of DMMP revealed a negligibly low influence of these steps on the kinetics of DMMP consumption. The measurements also showed that only $HOPO(CH_3)(OCH_3)$ was present in the flame in considerable amounts, while $HOPO(OCH_3)_2$ and $PO(CH_3)(OCH_3)(OCH_2)$ were not detected at all. Thus, the following route of DMMP destruction in the flame was proposed:[58]

$$PO(CH_3)(OCH_3)_2 + H\ (or\ OH) \longrightarrow$$
$$\longrightarrow HOPO(CH_3)(OCH_3) + CH_3\ (or\ OCH_3),$$
$$HOPO(CH_3)(OCH_3) + H\ (or\ OH) \longrightarrow$$
$$\longrightarrow (HO)_2PO(CH_3) + CH_3\ (or\ OCH_3),$$
$$(HO)_2PO(CH_3) + OH \longrightarrow (HO)_3PO + CH_3,$$
$$(HO)_3PO \longrightarrow \text{final products.}$$

The assumption that the reactions of DMMP with hydroxyl yield preferably methyl methylphosphonate rather than dimethyl phosphate is supported by the fact that the C–O bond energy is lower than the C–P bond energy. The mechanism of DMMP destruction proposed by

§ The same authors published a special study dealing with determination of the ionisation potentials of compounds $(CH_3)PO_2$ and $(CH_3O)PO_2$.[12]

Table 3. Reactions included in the Twarowski mechanism [2] and measured [58] parameters A, n and E of the equation $k = AT^n\exp(-E/RT)$.

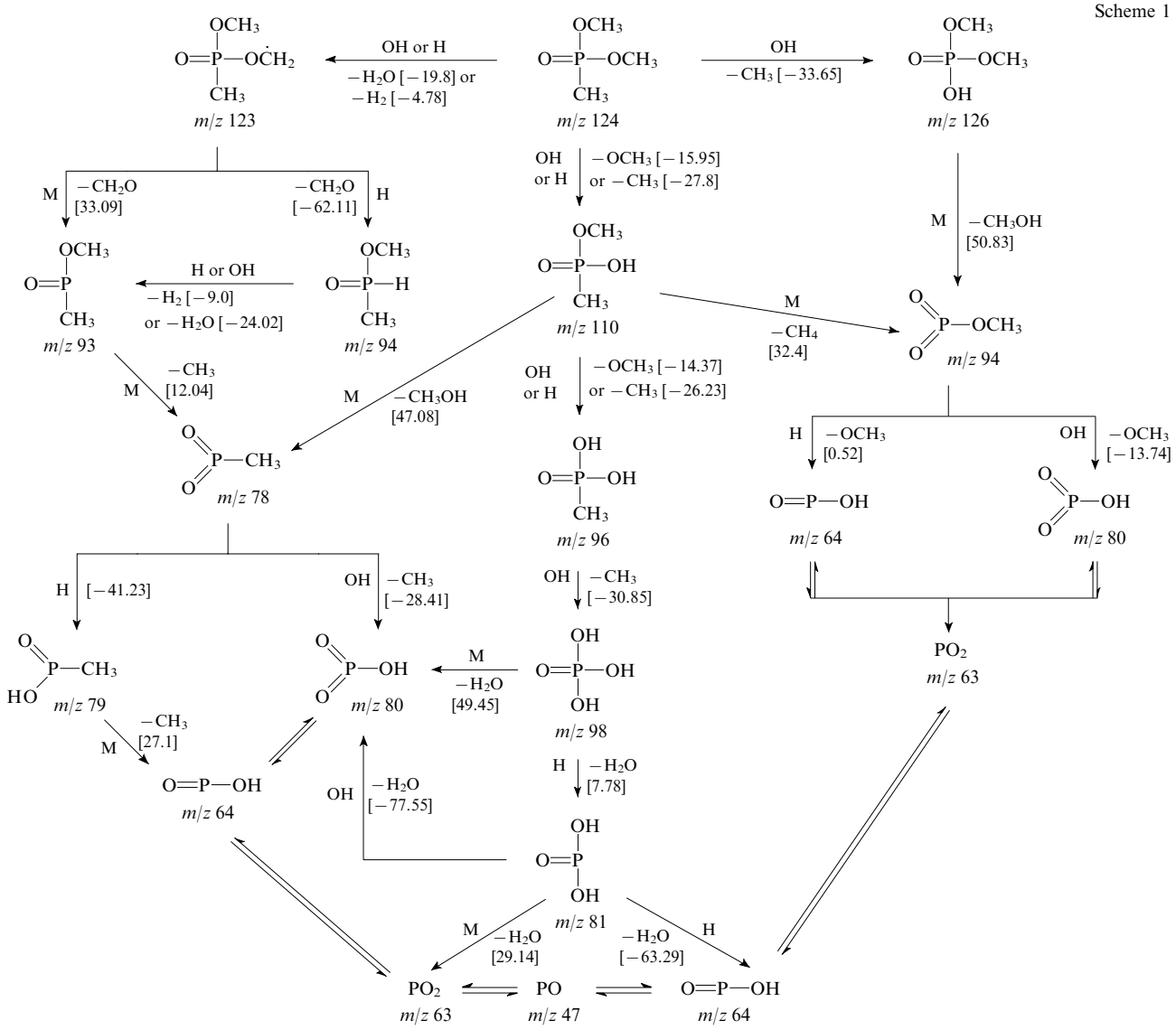
Number of the reaction	Reaction	A (from data of Ref. 2) [a]	A (from data of Ref. 58) [a]	n	E/kJ mol^{-1}
1	OH + PO + M = HOPO + M	1.196×10^{20}	1.19×10^{20}	−1.8	5.81
2	H + HOPO = H_2O + PO	3.16×10^{13}	6.32×10^{11}	0	49.87
3	OH + PO_2 + M = $HOPO_2$ + M	1.60×10^{24}	1.60×10^{25}	−2.3	1.19
4	H + $HOPO_2$ = H_2O + PO_2	3.16×10^{13}	6.32×10^{11}	0	49.87
5	H + PO_2 + M = HOPO + M	9.73×10^{23}	9.73×10^{24}	−2.0	2.7
6	OH + HOPO = H_2O + PO_2	3.16×10^{11}	3.16×10^{11}	0	0
7	H + HOPO = H_2 + PO_2	3.16×10^{13}	7.90×10^{11}	0	0.18
8	O + HOPO = OH + PO_2	3.16×10^{13}	1.58×10^{12}	0	0
9	OH + PO = H + PO_2	3.16×10^{11}	6.32×10^{10}	0	2.49
10	O + PO + M = PO_2 + M	2.36×10^{23}	2.36×10^{24}	−2.1	1.62
11	O_2 + PO = O + PO_2	3.16×10^{11}	3.16×10^{10}	0	23.91
12	OH + HOPO = H + $HOPO_2$	3.16×10^{11}	6.32×10^{10}	0	40.63
13	O + HOPO + M = $HOPO_2$ + M	1.59×10^{24}	7.95×10^{24}	−2.1	4.16
14	O + $HOPO_2$ = O_2 + HOPO	3.16×10^{13}	6.23×10^{11}	0	34.43
15	PO + $HOPO_2$ = PO_2 + HOPO	3.16×10^{11}	3.16×10^{11}	0	40.71

[a] The dimensionality of the pre-exponential factor A in the equation for the rate constant is s^{-1} for a unimolecular reaction, cm^3 mol^{-1} s^{-1} for a bimolecular reaction and cm^6 mol^{-2} s^{-1} for a trimolecular reaction.

Korobeinichev *et al.*[58] is presented in Scheme 1 (the corresponding reaction enthalpies are given in brackets).

The proposed mechanism of DMMP destruction in the flame was used to calculate the structure of a flame doped with 0.2 vol.% DMMP and the results of calculations were com-

Scheme 1



pared with the results of measurements. The agreement was satisfactory for almost all flame components. The concentration profiles of the following intermediates of DMMP destruction in the flame were reported:[58] methyl metaphosphate $(CH_3O)PO_2$, methyl methylphosphonate, methylphosphonic acid and orthophosphoric acid.

No direct calibration of an MBMS unit with respect to intermediate organophosphorus products of DMMP destruction was carried out, as these compounds are lacking, unstable or non-volatile (as, for example, methylphosphonic acid), and calibration with respect to orthophosphoric acid proved to be impossible, because this acid decomposed above 100 °C to give water and pyrophosphoric acid. Therefore, the calibration coefficients of the intermediate organophosphorus compounds in the flame were found using the procedure of equating the maximum measured and calculated concentrations, as this was done before (see Ref. 13).

It should be borne in mind that PO, PO_2, HOPO and $HOPO_2$ are formed in the flame at high temperature, while after cooling, the composition of combustion products may change appreciably (apparently, various phosphorus-containing acids may form).

2. Mechanism of trimethyl phosphate destruction

The mechanism of destruction of TMP in the flame, unlike that of DMMP, has been studied in detail.[15, 58, 64, 67–69] Mass spectra of the samples taken from the H_2/O_2/Ar flame doped with TMP exhibited peaks for the intermediate and final products of TMP destruction with m/z 80, 95, 96, 109, 110, 111, 112 and 126. The intensity profiles of some of these peaks and the TMP peak with m/z 140, recorded with IE = 21 eV, are presented in Fig. 4. Since the ion peak with m/z 126 is missing from the mass spectrum of TMP and its intensity profile passes through a maximum, this peak may be related to an intermediate of TMP destruction identified as dimethyl phosphate $HOPO(OCH_3)_2$ (DMP).

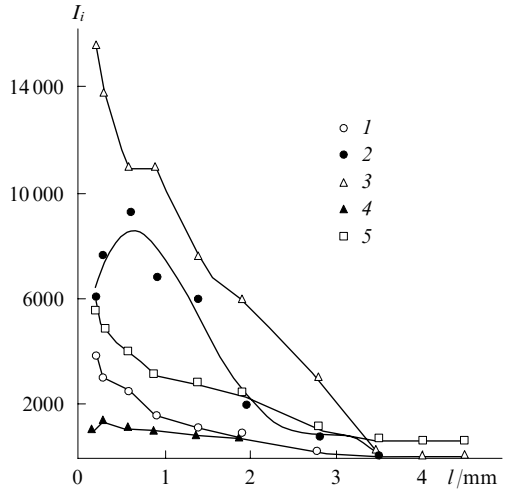


Figure 4. Intensity profiles of peaks of initial TMP (m/z 140) (curve *1*) and ions with m/z 126 (*2*), 110 (*3*), 109 (*4*) and 80 (*5*) in the H_2/O_2/Ar flame with 0.2 vol.% TMP at P = 47 Torr, IE = 21 eV.[14]

The mass spectra of tri- and dimethyl phosphates exhibit ion peaks with m/z 80, 95, 96, 109, 110, 111 and 112. Figures 5 and 6 present the intensity profiles of these peaks in the flame with subtracting the contributions of TMP and DMP. It can be seen from Fig. 6 that the profile of the ion peak with m/z 110 has three maxima, the third one being feebly pronounced and may be the result of overlap of two curves with maxima at

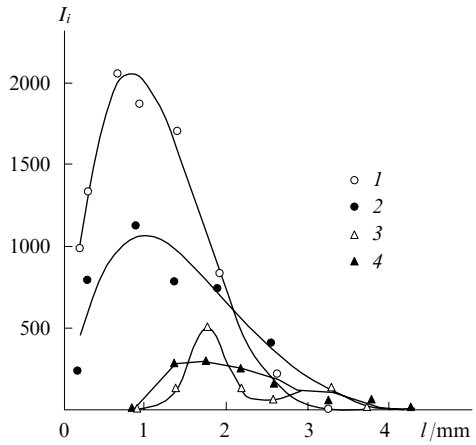


Figure 5. Intensity profiles of ion peaks with m/z 96 (curve *1*), 95 (*2*), 111 (*3*), 112 (*4*) with allowance for contributions of TMP and DMP fragment ions at P = 47 Torr in the H_2/O_2/Ar flame with 0.2 vol.% TMP.

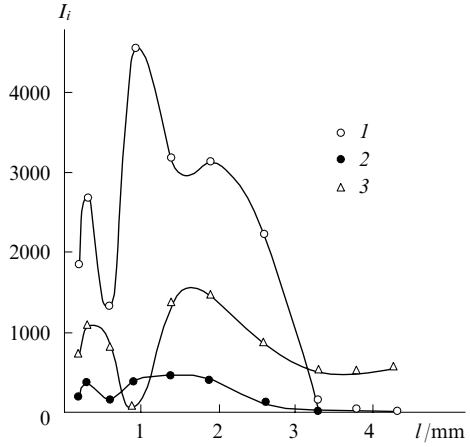


Figure 6. Intensity profiles of ion peaks with m/z 110 (curve *1*), 109 (*2*), 80 (*3*) with allowance for contributions of TMP and DMP fragment ions at P = 47 Torr in the H_2/O_2/Ar flame with 0.2 vol.% TMP.[14]

l = 1.1 and 1.9 mm. The ion with m/z 110 can be identified either as the molecular ion of dimethyl phosphonate $HPO(OCH_3)_2$ or dimethyl phosphite $HOP(OCH_3)_2$ or as the fragment ion formed from monomethyl phosphate $(HO)_2PO(OCH_3)$ (molecular mass 112). It can be seen from Figs 5 and 6 that the maximum of the ion peak with m/z 112 coincides with the third maximum of the m/z 110 peak. This prompted the conclusion that the third maximum of the m/z 110 peak corresponds to monomethyl phosphate, while the first one is due to dimethyl phosphite. The second maximum has not yet been interpreted. The peaks with m/z 80 and 109 were attributed to fragment ions formed from monomethyl phosphate and dimethyl phosphite. The ion peak with m/z 96 belongs apparently to monomethyl phosphite (the m/z 95 peak is due to a product of its fragmentation). The intensity profiles of ion peaks with m/z 47 (PO), 63 (PO_2), 64 (HOPO) and 80 ($HOPO_2$) in the flames with TMP and DMMP additives follow the same pattern.

On the basis of these data, possible reactions for TMP destruction in the flame were proposed. The kinetic model of TMP destruction based on these studies was verified in relation to different flames. The concentration profiles of the organophosphorus products of TMP destruction were constructed by

carrying out direct calibrations of an MBMS unit with respect to TMP, DMP and dimethyl phosphite.[64] Pure monomethyl phosphate was not obtained; therefore, its concentration was estimated from the phosphorus material balance for the flames. Apart from the transformation steps of TMP and the intermediate products of its combustion, which logically follow from analysis of the composition of the combustion products, the reactions of TMP with the OH radical were also considered. It was found that this reaction does not give dimethyl phosphate and methyl alcohol, as was considered previously, but gives water and organophosphorus radical resulting from elimination of the H atom from a TMP molecule.[70]

$$(CH_3O)_3PO + OH = (^{\bullet}CH_2O)(CH_3O)_2PO + H_2O$$

$$(\Delta H^{\circ}_{298} = -79.09 \text{ kJ mol}^{-1}).$$

The rate constant for this reaction was measured at a temperature of 300 K, and no activation energy was determined.[70] This was taken to be equal to the activation energy of a similar reaction of DMMP with OH,[13] *i.e.*, 16.7 kJ mol^{-1}. The pre-exponential factor in the Arrhenius equation was calculated proceeding from the accepted activation energy and the measured rate constant.[70] Thus, this reaction was included in the mechanism as a possible primary step of TMP destruction in the flame.

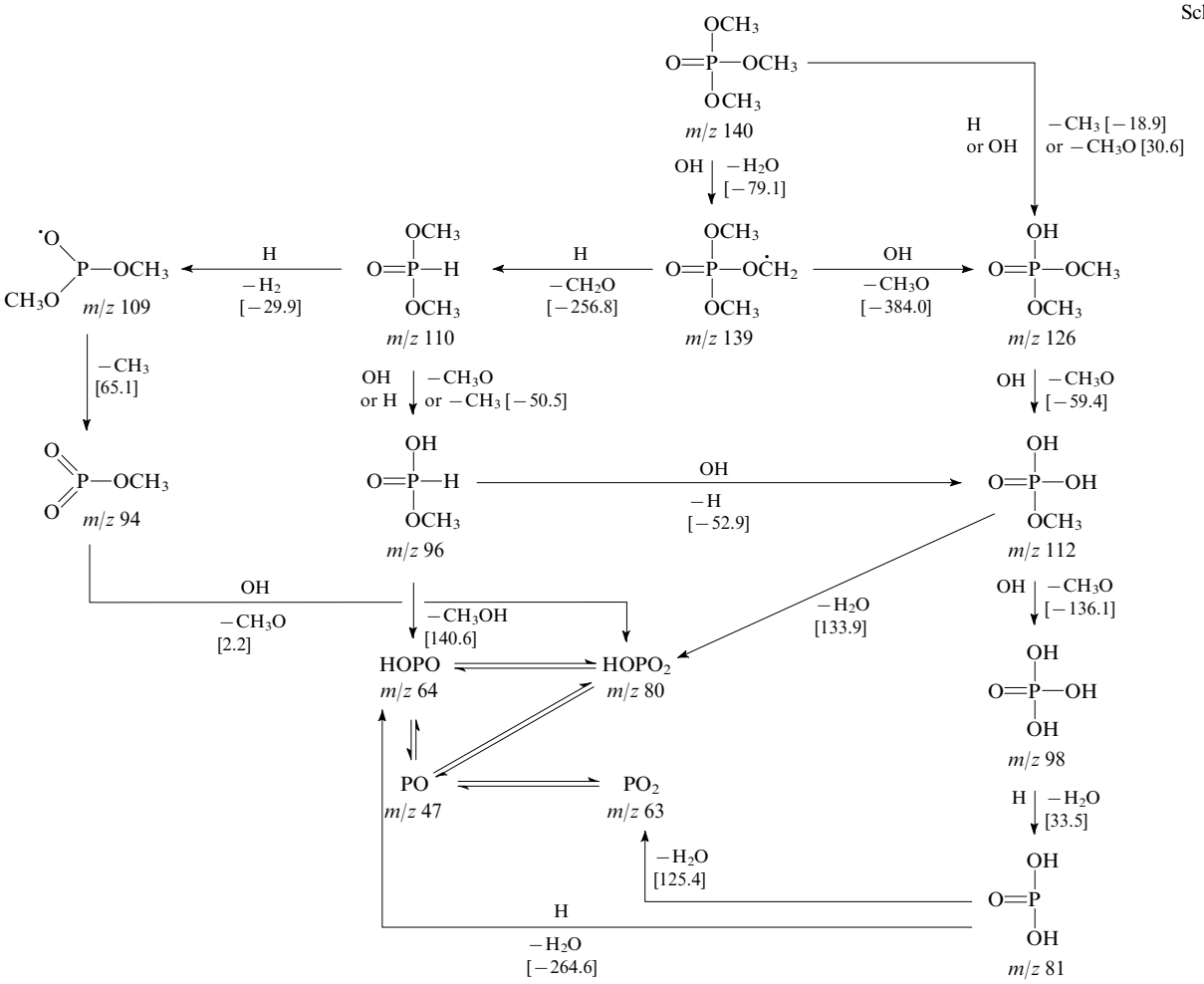
The mechanism of TMP destruction is presented in Scheme 2.[58, 64] It is of interest to carry out the integral analysis of the transformation routes of TMP and some products of its incomplete destruction to elucidate the role of each step. Analysis showed that the $(^{\bullet}CH_2O)(CH_3O)_2PO$ radical formation is a key step (consuming more than 70% of TMP), the main bulk of products being formed *via* this step. The proposed mechanism of TMP destruction was used to model the structure of the $H_2/O_2/Ar$ flame with a TMP additive.

Figure 7 presents the measured and calculated concentration profiles for TMP and intermediate organophosphorus products of its decomposition in the $H_2/O_2/Ar$ flame at low temperature. It can be seen from comparison of the calculated and experimental data that, despite certain discrepancies, the proposed [58] model predicts with a satisfactory accuracy the concentration profiles of intermediate organophosphorus products of the destruction of the starting compound. Figure 8 shows the calculated and measured concentration profiles of the final phosphorus-containing products of TMP combustion, namely, PO, PO_2, HOPO, $HOPO_2$ and $(HO)_3PO$. Satisfactory agreement between the simulated and experimental results was obtained. [The experimental and simulated results for stable substances (H_2, O_2, H_2O) are compared in Section IV.]

It follows from the series of studies devoted to the OPC combustion chemistry that predicting the concentration profiles of the combustion products PO, PO_2, HOPO and $HOPO_2$ using the kinetic model is the most complicated task, but these concentration profiles, in addition to the concentration profiles of the H and O atoms and OH radicals, allow one to find whether the mechanism correctly describes the OPC combustion, which is especially important for the description of OPC as combustion inhibitors (or promoters).

Original mechanisms for DMMP and TMP destruction in the flames based on quantum chemical calculations of thermochemical data and on the estimation of rate constants for separate steps were proposed almost simultaneously by two

Scheme 2



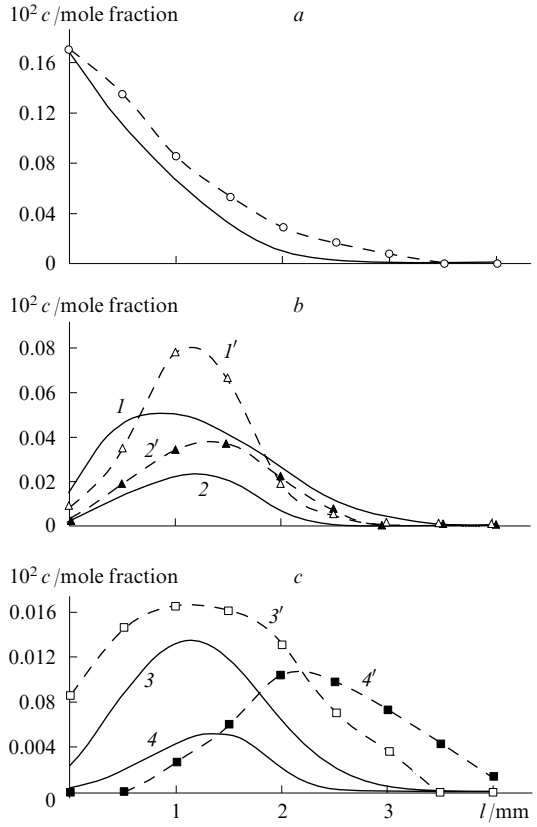


Figure 7. Concentration profiles of TMP (*a*) and intermediate products of its destruction: phosphites (*b*) and phosphates (*c*) in the $H_2/O_2/Ar$ flame.[58]
The dots show the experimental values and the continuous lines correspond to calculations;
(*b*) (*1*, *1′*) dimethyl phosphite; (*2*, *2′*) monomethyl phosphite;
(*c*) (*3*, *3′*) dimethyl phosphate; (*4*, *4′*) monomethyl phosphate.

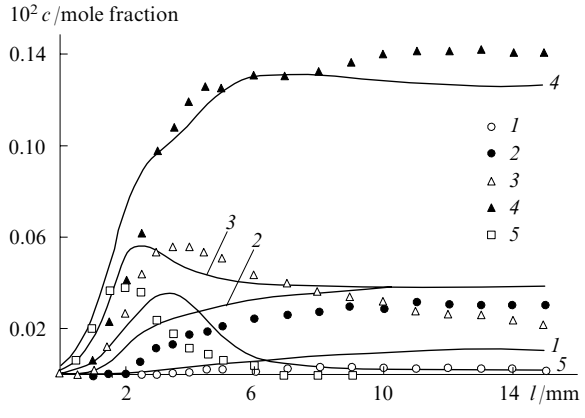


Figure 8. Concentration profiles of phosphorus-containing products of TMP combustion in the $H_2/O_2/Ar$ flame.[58]
Phosphorus-containing products: PO (curve *1*), PO_2 (*2*), HOPO (*3*), $HOPO_2$ (*4*), $(HO)_3PO$ (*5*). The dots show the experimental values and the continuous lines correspond to calculations.

research groups.[52, 54] (Glaude *et al.*[54] took into account all the possible intermediates of destruction of these OPC.) The developed mechanisms were used to simulate the structure of the low-pressure hydrogen–oxygen flame doped with 0.2 vol.% DMMP or TMP. A comparison of the calculation results[54] with earlier experimental results[64, 69] demonstrated good agreement between them as regards both the concentrations of stable components in the flame (H_2, O_2 and H_2O) and the concentrations of PO, PO_2, HOPO, $HOPO_2$ and $(HO)_3PO$, which is the most difficult-to-attain fitting criterion. At that time, the developed mechanism was the most complete (it included 202 reactions involving 41 phosphorus compounds). This mechanism served as the basis for the development of the mechanism of inhibition of methane and propane flames by OPC additives under atmospheric pressure (see below).

3. Mechanism of destruction of diisopropyl methylphosphonate and sarin

The chemistry of DIMP combustion in the H_2/O_2 flame at low pressure has been studied.[71] Diisopropyl methylphosphonate decomposes rather readily, unlike TMP or DMMP, when heated in an inert gas flow; therefore the thermal decomposition reactions were included in the mechanism of DIMP destruction in the flame. The kinetics and the products of DIMP pyrolysis in a flow type reactor were studied by Zegers and Fisher;[72] the results are presented below.

$$(\text{iso-}C_3H_7O)_2(CH_3)PO + M \xrightarrow[[82.3\ \text{kJ mol}^{-1}]]{}$$

$$\longrightarrow (\text{iso-}C_3H_7O)(CH_3)PO(OH) + C_3H_6\,,$$

$$k = 10^{12}\exp\left(\frac{-153.4 \pm 20}{RT}\right)\ \text{cm}^3\ \text{mol}^{-1}\ \text{s}^{-1}.$$

While estimating the contribution of thermal decomposition of DIMP to the overall destruction rate of the substance in the flame, it was concluded[72] that thermal decomposition plays a minor role in the total mechanism of DIMP destruction. As in the case of other OPC, the major steps of DIMP destruction include the reactions of the OPC molecule with the H atom and OH radical, resulting in replacement or elimination of the CH_3 and C_3H_7O groups, respectively.

By analogy with the DIMP destruction steps, Korobeinichev *et al.*[71] proposed also the possible steps of sarin destruction. They carried out altogether 10 reactions and calculated the heats of reactions based on the Melius thermochemical data (the Lawrence Livermore National Laboratory).

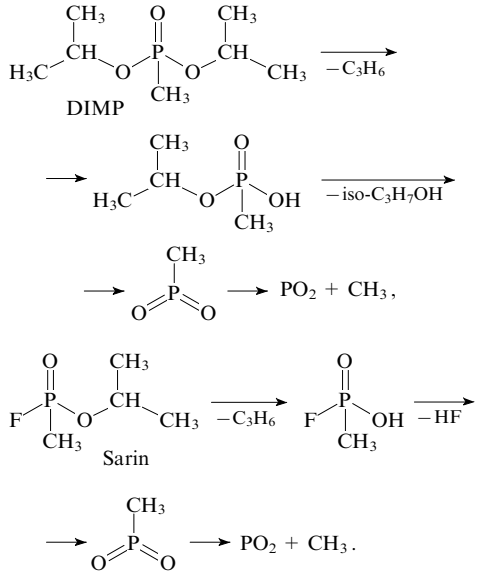
The rate constants for unimolecular decomposition of dimethyl ethylphosphonate, triethyl phosphate and DIMP were calculated.[54] The correctness of calculations was verified by comparing the simulation data with the experimental results on the pyrolysis of the above-mentioned OPC in a flow type reactor.

As a continuation of their research, the same group[73] developed the destruction mechanisms for a number of fluorinated OPC and TMP, DMMP, DIMP and sarin. The hierarchical schemes of reactions were based on previously proposed mechanisms of OPC destruction using the principle of chemical bond additivity. The kinetic models of combustion of the above-listed OPC and sarin were used in the calculations predicting their consumption rates during the combustion of natural gas (94% of methane and 6% of ethane) with air in a perfect-mixing reactor.¶ A comparison of the dependences of concentrations of various OPC in the combustion on temperature and residence time has shown that TMP and DMMP consumption follow identical kinetics; the same is true for DIMP and sarin. The researchers concluded that only DIMP is a true mimic of sarin.

Scheme 3 shows simplified patterns of the thermal destruction of DIMP and sarin at high temperature in a perfect-mixing

¶ This process simulates disposal of these compounds by incineration in a furnace.

Scheme 3



reactor. It is noteworthy that both DIMP and sarin destruction mechanisms include not only thermal decomposition steps. A full mechanism of sarin combustion that includes 24 steps most of which are reactions of sarin with H and OH radicals has been reported.[73]

Comparative analysis of the mechanisms of destruction of various OPC carried out by the researchers cited has shown that the six-centred elimination of C_3H_6 present in the destruction mechanisms of DIMP and sarin is responsible for their higher reactivity compared to that of TMP or DMMP. This means that C—C bonds are most susceptible to cleavage in the OPC molecule.

It is noteworthy that the conclusions drawn[73] are at variance with the conclusions of an earlier publication.[71] As noted above, experimental study and numerical simulation of the DIMP destruction mechanism in the low-pressure hydrogen–oxygen flame [71] led to the conclusion that the thermal decomposition of DIMP gives a minor contribution to the overall destruction rate. Apparently, these discrepancies can be interpreted in the following way. The concentrations of H, O and OH atoms and radicals in the hydrogen–oxygen flame at low pressure are very high (according to a publication,[74] the H + O + OH molar concentration is about 10%). This suggests that the role of thermal decomposition of even thermally unstable compounds is negligibly low against the high rate of DIMP consumption in reactions with the H, O and OH radicals. In hydrocarbon flames, the total molar concentration of active species was reported [75] to be two orders of magnitude lower. In this case, the role of thermal decomposition markedly increases.

4. Mechanism of destruction of organophosphorus compounds in a non-thermal plasma

The mechanisms of OPC destruction in the flame and non-thermal plasma have much in common. Therefore, it is pertinent to consider briefly the works devoted to the chemistry of OPC destruction in corona discharge plasma. From the practical standpoint, the non-thermal plasma attracts attention of researchers as a medium for effective destruction of toxic or hazardous compounds in low concentrations.

The identification of the OPC destruction products in a non-thermal plasma [76–78] made it possible to propose the mechanism of their destruction. Among the stable intermediate products of DMMP destruction in the corona discharge plasma, methyl methylphosphonate and monomethyl phosphate were detected; methylphosphonic and orthophosphoric acids were formed as the final products of DMMP destruction. The same species are also the final products of DIMP destruction, whereas isopropyl methylphosphonate is an intermediate product. The destruction of TMP yields dimethyl and monomethyl phosphates (intermediates) and orthophosphoric acid (final product).

Thus, in a non-thermal plasma, DMMP, DIMP and TMP undergo the following transformations:

DMMP: $(CH_3O)_2(CH_3)PO \longrightarrow (CH_3O)(HO)(CH_3)PO \longrightarrow$
$\longrightarrow (CH_3O)(HO)_2PO \longrightarrow (HO)_2(CH_3)PO \longrightarrow (HO)_3PO$;

DIMP: $(iso\text{-}C_3H_7O)_2(CH_3)PO \longrightarrow$
$\longrightarrow (iso\text{-}C_3H_7O)(HO)(CH_3)PO \longrightarrow$
$\longrightarrow (HO)_2(CH_3)PO \longrightarrow (HO)_3PO$;

TMP: $(CH_3O)_3PO \longrightarrow (CH_3O)_2(HO)PO \longrightarrow$
$\longrightarrow (HO)_2(CH_3O)PO \longrightarrow (HO)_3PO$.

The identification of the OPC decomposition products in a non-thermal plasma showed that they are the same as many OPC destruction products in the flame. Apparently, in a corona discharge, as in the flame, the alkoxyl and alkyl groups are replaced successively by H or OH. Two possible mechanisms of OPC destruction in the nonthermal plasma, radical and ionic ones, have been described. According to the radical mechanism, OPC destruction occurs upon the reaction of the atoms and radicals formed in the discharge with OPC, similarly to the situation in the flame. The discussion of the ionic mechanism in the OPC destruction in the nonthermal plasma is beyond the scope of this review. It should be noted that no unambiguous evidence supporting either of these two mechanism is currently available.

IV. Mechanism of promotion and inhibition of the H_2/O_2 flames by addition of organophosphorus compounds

Korobeinichev *et al.*[14, 57, 64] first demonstrated experimentally that the addition of 0.2 vol.% OPC to the $H_2/O_2/Ar$ flames at low pressure results in an increase in the final temperature of the flame and the degree of combustion and in a decrease in the combustion zone width. Figure 9 shows the measured and calculated (at a 15 mm distance from the burner) final temperatures of the $H_2/O_2/Ar$ flame stabilised on a flat burner at 47 Torr, depending on the initial concentration of the TMP additive.[79] Under these conditions, the increase in temperature

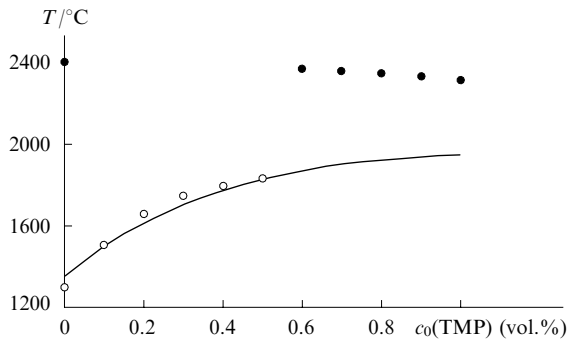


Figure 9. Maximum temperature of the $H_2/O_2/Ar$ flame stabilised on a flat burner at a pressure of 47 Torr *vs.* TMP concentration.[79]
The continuous line shows the calculated values; the light dots are experimental values and the dark dots show the change in the adiabatic equilibrium temperature.

of the stabilised flame is not related to lower heat loss in the burner, as is usually the case upon the addition of inhibitors; conversely, on the addition of TMP, the flame temperature increases simultaneously with the increase in the temperature gradient at the burner surface, *i.e.*, with an increase in the heat loss. Thus, the increase in the flame temperature with an increase in the TMP concentration is due not to the introduction of additional fuel into the flame but to more complete combustion of the fuel already present as a result of the ability of OPC combustion products to catalyse recombination of the H and OH radicals to give water, *i.e.*, to promote combustion.

The experimental and simulation results are in satisfactory agreement, which confirms the consistency of the kinetic model. For comparison, Fig. 9 shows also the equilibrium temperatures of the adiabatic flames with the same composition. The difference between the adiabatic flames and flames stabilised on a flat burner (cooled) is that in the latter case, a large portion of heat is absorbed by the burner.

Figure 10 shows the concentration profiles of the stable components H_2, O_2 and H_2O in the $H_2/O_2/Ar$ flame stabilised on a flat burner at a reduced pressure of 47 Torr without additives or with 0.2 vol.% TMP.[66] The narrowing of the combustion zone (the final composition of the combustion products is attained at a shorter distance from the burner surface) and fuller combustion of the H_2 and O_2 components attest to a promoting effect of TMP on the flame.

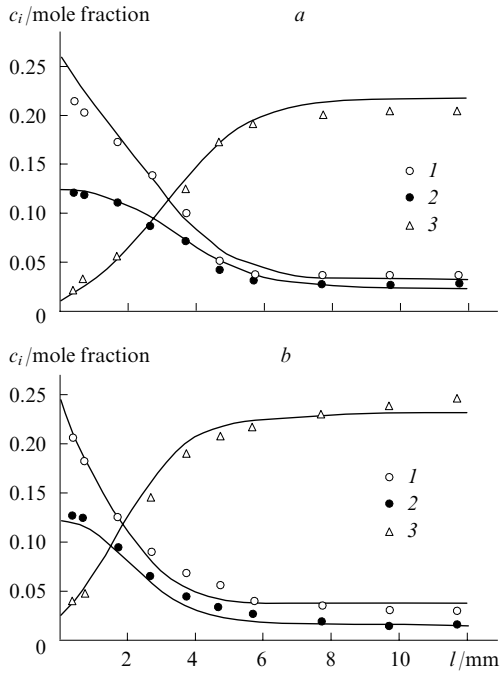


Figure 10. Concentration (c_i) profiles of stable components H_2 (*1*), O_2 (*2*) and H_2O (*3*) in the $H_2/O_2/Ar$ flame stabilised on a flat burner at $P = 47$ Torr without additives (*a*) and with 0.2 vol.% TMP (*b*).[66]
The dots show experimental values and the lines correspond to simulation results.

The observed promoting effect was confirmed by comparing experimental data with simulation results obtained using the mechanism proposed by Glaude *et al.*[54] The promoting effect of OPC increases with an increase in the concentration and reaches a maximum at an OPC concentration of $\sim$0.6 vol.%. This can be seen from the computational data presented in Fig. 11, which shows the dependence of the free propagation speed of the hydrogen–oxygen flame on the additive concentration at a reduced pressure (47 Torr). In the

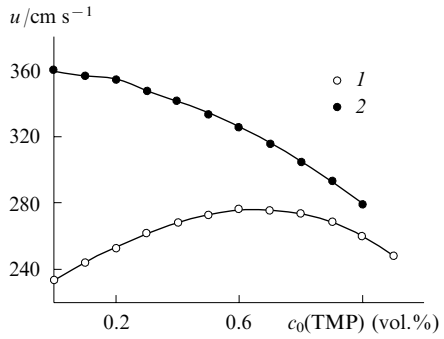


Figure 11. Normal propagation speed of the H_2/O_2 flames *vs.* the concentration of TMP additive at pressures of 47 (curve *1*) and 760 Torr (curve *2*).

TMP concentration range from 0 vol.% to 0.6 vol.%, this additive acts as a promoter. On further increase in the TMP concentration, the flame propagation speed decreases. At a pressure of 760 Torr (1 atm), OPC acts only as an inhibitor.

The effect of OPC on the concentration of the H, O and OH radicals in the flame is shown in Fig. 12, which gives the calculated and measured concentrations of these radicals in the $H_2/O_2/Ar$ flame without additives and with 0.2 vol.% TMP.[66] The introduction of OPC results in a decrease in the concentration of hydrogen and oxygen atoms and an increase in the hydroxyl concentration. It can be seen

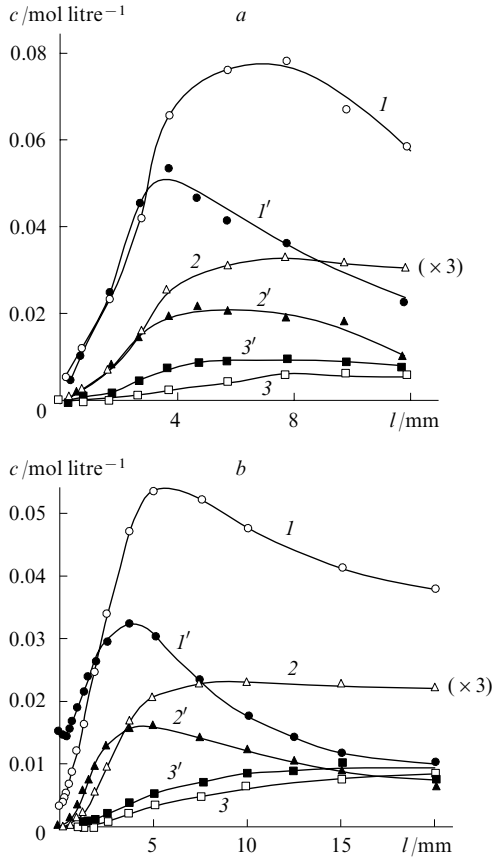


Figure 12. Concentration profiles of radicals H (curves *1*, *1′*), O (*2*, *2′*) and OH (*3*, *3′*) in the $H_2/O_2/Ar$ flame stabilised on a flat burner at $P = 47$ Torr without an additive (light dots) and with 0.2 vol.% TMP (black dots).[66] (*a*) experimental data, (*b*) simulation results.

from comparison of the concentration profiles that the computation and experimental results are in satisfactory agreement. The effect of OPC on the concentrations of H, O, and OH radicals is an important feature of these compounds, which accounts for their possible practical application as combustion inhibitors and flame suppressants.

It was shown[69] that the addition of OPC to a methane–oxygen flame at a pressure of 0.1 bar decreases the flame propagation speed. Thus, OPC are combustion promoters only for low-pressure hydrogen flames. Note that an increase in the propagation speed of flames with an increase in the concentration of the inhibitor (bromoethane, dibromotetrafluoroethane, bromine, diethylamine, methane, and methanol) in lean and rich hydrogen–air flames at high pressures was described previously.[80] However, the mechanism of this effect is different and is related, in the authors' opinion, to the fact that active additives can function as additional fuel or oxidant.

The additional heat release caused by combustion of the additive (at a definite concentration) can counterbalance its inhibiting action. However, the action of OPC is due to a kinetic rather than thermophysical effect. The H and OH radical recombination in the flame catalysed by OPC destruction products is yet another channel for water formation

$$HO + PO_2 + M = HOPO_2 + M,$$

$$H + HOPO_2 = H_2O + PO_2,$$

which provides heat release. The evolved heat increases the temperature and accelerates recombination of active species, despite the decrease in their concentration in the flame.

A detailed interpretation of the promoting effect of OPC based on the analysis of the kinetic model of OPC destruction (see Ref. 58) has been proposed.[79,81] The calculations of the quadratic branching rate

$$H + O_2 = OH + O \ (E_{act} = 61.8 \text{ kJ mol}^{-1}) \quad (1)$$

for the combustion zone of a hydrogen–oxygen flame at low pressure showed that the rate of this reaction considerably increases with an increase in the TMP concentration and reaches a maximum at $c_{TMP} = 0.5$ vol.%.–0.6 vol.%. This increase in the reaction rate is mainly due to an increase in the flame temperature † as a result of increase in the recombination rate of H, O and OH atoms and radicals. The quadratic branching rate stops to grow following an increase in the TMP concentration where the flame temperature reaches an equilibrium.

A comparison of contributions of various reactions to the flame propagation speed demonstrated that with an increase in the TMP concentration, the contribution of branching exceeds considerably the contributions of reactions (2)–(5) contained in the hydrogen oxidation mechanism (Fig. 13).

$$OH + H_2 = H_2O + H, \quad (2)$$

$$O + H_2 = OH + H, \quad (3)$$

$$H + O_2 + M = HO_2 + M, \quad (4)$$

$$H + HO_2 = 2\,OH. \quad (5)$$

The increase in the branching rate with an increase in the TMP concentration and saturation of this effect as the flame temperature approaches the equilibrium value is shown in Fig. 14. Among reactions involving phosphorus-containing

† The rate of branching reaction, which is proportional to the product of H atom concentration by the rate constant for the reaction, increases with an increase in the TMP concentration owing to the fact that the reaction rate constant grows (with an increase in temperature) faster than the H concentration drops.

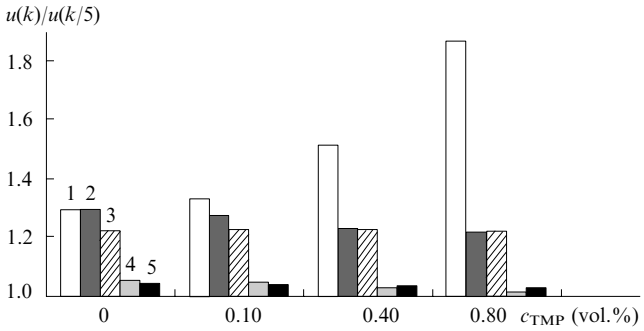


Figure 13. Sensitivity coefficients $[u(k)/u(k/5)]$ of reactions (1)–(5) taking place in the flame comprising 26% H_2 + 13% O_2 + 61% Ar at $P = 47.5$ Torr and $T_0 = 370$ K for different TMP concentrations;[81] $u(k)$ is the flame propagation speed calculated with the standard rate constant for the reaction; $u(k/5)$ is the rate calculated with the rate constant decreased fivefold.

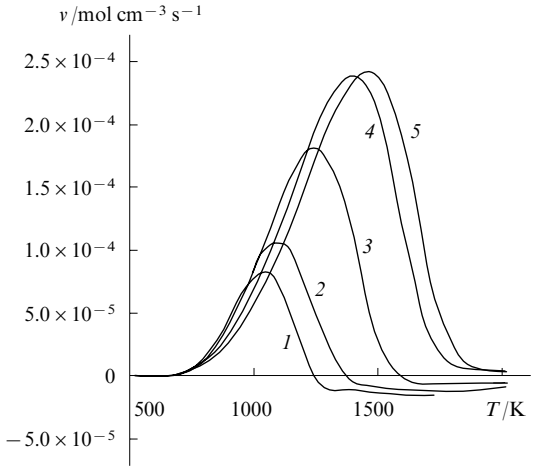


Figure 14. Rate constant for quadratic branching $H + O_2 = OH + O$ as a function of temperature of the flame comprising 26% H_2 + 13% O_2 + 61% Ar without additives (curve *1*) and with TMP (curves *2*–*5*) added in different concentrations at $P = 47.5$ Torr and $T_0 = 370$ K.[81]
c_{TMP} (%): 0.1 (*2*), 0.4 (*3*), 0.8 (*4*), 1.0 (*5*).

compounds to which the flame propagation speed is most sensitive (according to Ref. 81), the following reactions should first be noted:

$$OH + PO_2 + M = HOPO_2 + M, \quad (6)$$

$$H + PO_2 + M = HOPO + M, \quad (7)$$

$$O + HOPO = OH + PO_2, \quad (8)$$

$$H + HOPO_2 = H_2O + PO_2, \quad (9)$$

$$H + HOPO = H_2 + PO_2. \quad (10)$$

These reactions result in chain termination and play an important role in the catalytic radical recombination cycle. The calculation of the sensitivity coefficients of the flame propagation speed to the reaction rate constants for flames with different OPC concentrations has shown that in the additive concentration range from 0 vol.% to 0.5 vol.%, these coefficients are positive, *i.e.*, recombination reactions increase the flame propagation speed. When the TMP concentration is > 0.5 vol.%, the coefficients are negative and decrease with an increase in the OPC concentration in the flame, *i.e.*, the

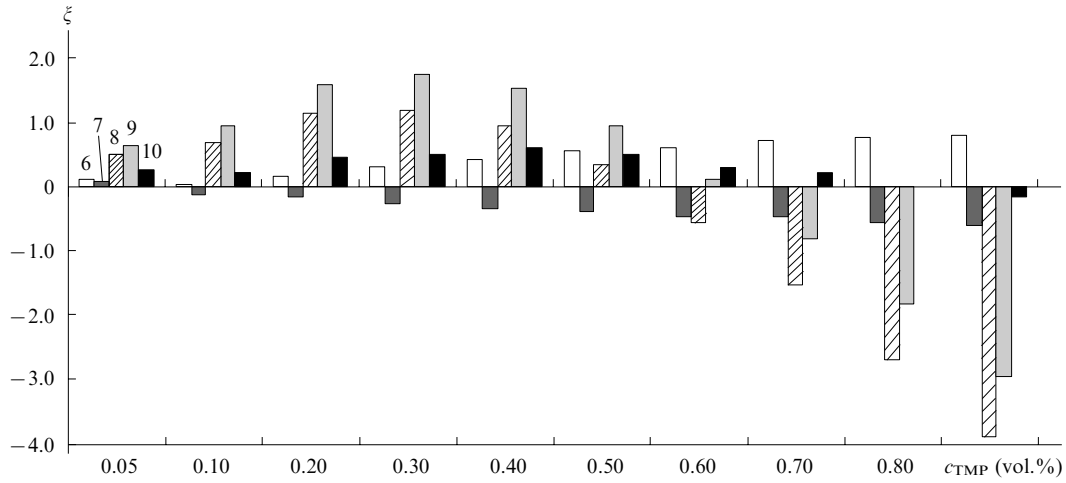


Figure 15. Sensitivity coefficients of key reactions (6)–(10) taking place in the $H_2/O_2/Ar$ flame with participation of OPC for different TMP concentrations.[81]

hydrogen combustion is retarded. Thus, transition from promotion to inhibition with the same reactions being responsible for this attests to unique properties of phosphorus compounds. Figure 15 presents the sensitivity coefficients (ξ) for the key reactions that take place in the flame and involve phosphorus-containing compounds at different TMP concentrations. The sensitivity coefficients were determined from the relation

$$\xi = \frac{u(k) - u(k/5)}{u(k)}\ 100\%,$$

where $u(k)$ is the free propagation speed of the $H_2/O_2/Ar$ flame with a TMP additive at a pressure of 47.5 Torr; $u(k/5)$ is the free propagation speed of the flame calculated using the reaction rate constant reduced fivefold.

Under atmospheric pressure, the concentration of active species in the flame is two orders of magnitude lower than under reduced pressure, and the temperature of the adiabatic flame is close to thermodynamic equilibrium; therefore, even a minor additive of phosphorus compounds results only in flame inhibition.

The chemistry of combustion of sulfur and nitrogen compounds is similar to the phosphorus combustion chemistry. The inhibiting action of SO_2 on the hydrogen–oxygen flame stabilised on a flat burner has been studied.[82] The reactions

$$H + SO_2 + M = HOSO + M,$$

$$H + HOSO = H_2 + SO_2,$$

which play the key role in the inhibition mechanism and form the inhibition cycle, are similar to the reactions of phosphorus oxides and phosphorus-containing acids. However, the inhibiting efficiency of sulfur compounds is much lower compared to phosphorus. This can be attributed to the lower rates of catalytic reactions.

A computational theoretic analysis of the effect of nitrogen oxide admixture on the ignition delay in a hydrogen–air mixture has been carried out.[83] The calculations showed that at temperatures above 1200 K, the addition of NO to a hydrogen–air mixture somewhat decreases the ignition delay, *i.e.*, NO functions as a promoter. However, at lower temperature, the ignition delay increases, *i.e.*, the NO admixture functions as an inhibitor. The researchers believe that the effect of nitrogen oxide on the hydrogen oxidation kinetics is due to its ability to catalyse radical recombination

$$H + NO + M \longrightarrow HNO + M,$$

$$HNO + H \longrightarrow H_2 + NO,$$

$$HNO + OH \longrightarrow H_2O + NO.$$

These reactions are analogous to those presented for OPC.

V. Studies of the mechanism of inhibition and quenching of hydrocarbon flames by organophosphorus additives

1. Premixed laminar flames

a. The structure of flames with organophosphorus additives

The work of Hastie and Bonnell,[6] who studied the effect of the classical inhibitor CF_3Br and of TMP on the methane–oxygen and hydrogen–oxygen flames of various types and compositions by molecular-beam mass spectrometry and optical methods, should be considered the pioneering study dealing with the effect of OPC on the combustion processes under atmospheric pressure. The visual monitoring of the height of the flame cone stabilised on the Bunsen burner allowed them to draw the first conclusion that the introduction of a TMP additive resulted in a decrease in the normal free propagation speed of the methane–oxygen flame, *i.e.*, they demonstrated that TMP is a combustion inhibitor. Hastie and Bonnell [6] were the first to propose a series of reactions involving phosphorus compounds (phosphorus oxides and phosphorus-containing acids), which described recombination of H and OH radicals. This was actually the first interpretation of the mechanism of flame inhibition by OPC.

Numerous experimental data collected by these researchers are unique and highly important. The key result of their studies is the discovery of the change in the concentrations of H, O and OH radicals upon the introduction of TMP into the flame. Hastie and Bonnell [6] obtained the first experimental proof for the existence of a relationship between the addition of TMP and the decrease in the concentration of active species in the flame. They measured the intensity profiles for ion peaks of PO, PO_2 and HPO_2 in the mass spectra. Noteworthy also is Hastie's contribution to the molecular-beam mass spectrometry studies of the behaviour of PO, PO_2 and $HOPO_2$ in the flames.[84] However, his paper [84] presents no consistent quantitative experimental data that could be compared with simulation results to verifiy the proposed inhibition mechanism. This study seems not to be completed as yet, because the results

were presented only in a report[6] and were not published in refereed editions.

Korobeinichev *et al.*[85] measured experimentally the concentration profiles of phosphorus oxides and phosphorus-containing acids in the methane–oxygen flames with TMP additive at a pressure of 1 atm and determined the dependences of the flame propagation speed on the additive concentration. A comparison of the results thus obtained with the data of simulation of the flame structure and propagation speed in terms of the mechanism proposed for the low-pressure flame[58] showed a discrepancy between the simulation and experimental results. Analysis of the sensitivity of flame propagation speeds to the change in the rate constants for PO-, PO_2-, HOPO- and $HOPO_2$-involving reactions and the effect of these reactions on the concentrations of phosphorus-containing products in the flame prompted the necessity of changing the pre-exponential factor in the expression for the rate constants for some key steps in the mechanism proposed by Korobeinichev *et al.*[58]

Considerable progress in the understanding of processes that take place in the flames with OPC additives was attained owing to quantum chemical calculations,[55] which resulted in upgrading of the Twarowski mechanism of flame inhibition by organophosphorus compounds. By computation of the potential energy surfaces for the transformations

$$HOPO + H = PO + H_2O,$$

$$HOPO_2 + H = PO_2 + H_2O,$$

which were earlier regarded as elementary steps,[54] Mackie *et al.*[55] demonstrated that actually these reactions occur in two steps:

$$HOPO + H \longrightarrow (HO)_2P \longrightarrow PO + H_2O,$$

$$HOPO_2 + H \longrightarrow (HO)_2PO \longrightarrow PO_2 + H_2O.$$

The subsequent calculation of the potential energy surfaces using more advanced methods[52, 53] demonstrated that these reactions may include even more steps:

$$HOPO + H \rightleftharpoons HOP(H)O \rightleftharpoons (HO)_2P \longrightarrow PO + H_2O,$$

$$HOPO_2 + H \rightleftharpoons HOP(O)(H)O \rightleftharpoons (HO)_2PO \longrightarrow PO_2 + H_2O.$$

According to the calculation,[53] the rate constant for the latter reaction at a temperature of 1500 K was 10 times higher than the value proposed previously.[54] Figure 16 shows the potential energy surfaces for the possible paths of the $HOPO_2 + H$ reaction. On the basis of quantum chemical calculations of the rate constants for some reactions and calculation of the thermochemical properties of phosphorus-containing molecules and transition states, the most complete and currently substantiated mechanism of flame inhibition by OPC additives under atmospheric pressure was developed at the Lawrence Livermore National Laboratory.[86] This mechanism includes

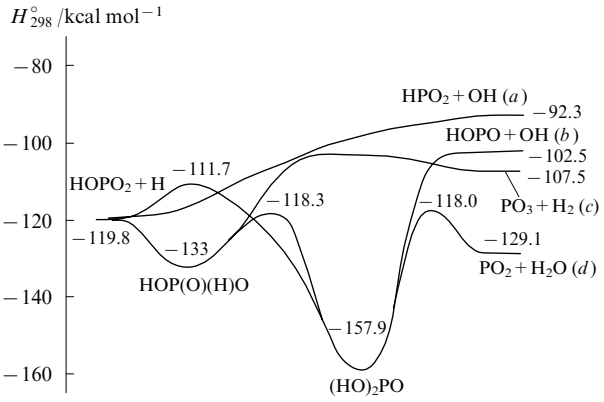


Figure 16. Potential surfaces of the possible transformation paths of the system $HOPO_2 + H$ (paths *a*–*d*) and the reaction products of $HOPO_2$ with H.[53]
The enthalpies of formation (in kcal mol^{-1}) for compounds and transition states are given.

210 steps involving 43 compounds. Apart from the above-considered steps, the steps involving compounds like P_2O_n and reactions of phosphorus oxides with alkyl radicals such as CH_3 and C_2H_5 were also included. The subsequent analysis showed that these steps do not have a significant effect on the results of flame simulation over a wide range of equivalence ratio. Thus, this mechanism can be considered even somewhat excessive.

The mechanism of flame inhibition by OPC additives can conventionally be divided into two parts. The first part includes destruction of OPC (TMP and DMMP) to 'light' phosphorus-containing compounds like $H_xP_yO_z$; the second one includes reactions of $H_xP_yO_z$ with the H, O and OH radicals, which ensure their removal from the flame through their catalytic recombination. This part of the mechanism is crucial in the description of flame inhibition phenomena by OPC additives. Table 4 presents the reactions from the second part of the mechanism and the corresponding rate constants. The notes to the Table outline the methods used to estimate the rate constants.

Note that Jayaweera *et al.*[53] made considerable advances not only in the development of the proper mechanism but in the in-depth understanding of processes taking place in the flames with OPC additives. They estimated the efficiency of action of inhibitors on the premixed flames using two parameters: the change in the concentrations of the H and OH radicals and the flame propagation speed. Both parameters were discussed for lean and rich flames with equivalence ratio $\phi = 0.8$ and 1.3, respectively.

It was mentioned above that the addition of OPC inhibits flame propagation by accelerating the recombination of H and OH radicals; therefore, the distribution of concentrations of

Table 4. Reactions of the key components in the flame with 'light' phosphorus-containing compounds $H_xP_yO_z$ and their rate constants [the rate constant is presented as $AT^n\exp(-E_a/RT)$, the pre-exponential factor A is expressed in s^{-1}, litre mol^{-1} s^{-1} or litre^2 mol^{-2} s^{-1}].

Number of the reaction	Reaction	A	n	E_a /J mol^{-1}	Notes
1	$PO_2 + PO + M = P_2O_3 + M$				calculation data
	high pressure	4.00×10^{14}	−1.00	0	
	low pressure	1.00×10^{20}	−2	0	
2	$PO_2 + PO_2 + M = P_2O_4 + M$				the same
	high pressure	6.00×10^{14}	−1	0	
	low pressure	2.00×10^{20}	−2	0	
3	$PO_2 + PO_3 + M = P_2O_5 + M$				"
	high pressure	6.00×10^{14}	−1	0	
	low pressure	5.00×10^{20}	−2	0	

Table 4 (continued).

Number of the reaction	Reaction	A	n	E_a /J mol^{-1}	Notes
4	$PO_2 + OH + M = HOPO_2 + M$ (low pressure) [b]	1.60×10^{24}	−2.28	1193.8	see [a]
5	$PO_3 + H + M = HOPO_2 + M$ (high pressure) [b]	4.80×10^{24}	−2.37	5977.4	"
6	$HOPO + O + M = HOPO_2 + M$ (high pressure) [b]	1.20×10^{27}	−2.99	8527.2	see [a]
7	$PO_3 + H_2 = HOPO_2 + H$	2.00×10^{12}	0	0	see [c]
8	$HOPO + OH = PO_2 + H_2O$	3.72×10^{13}	−0.22	13401.08	see [d] (date from Ref. 55)
9	$HOPO_2 + H = PO(OH)_2$	1.27×10^{32}	−6.10	36391.08	see [e]
10	$HOPO_2 + H = PO_2 + H_2O$	5.16×10^{19}	−1.83	44726	"
11	$PO(OH)_2 = PO_2 + H_2O$	1.45×10^{28}	−4.97	186678.8	"
12	$HPO_2 + OH = PO(OH)_2O$	1.00×10^{19}	−2	0	calculation data
13	$PO(OH)_2O + H = HOPO_2 + H_2O$	2.00×10^{13}	0	0	the same
14	$PO(OH)_2 + H = HPO_2 + H_2O$	4.00×10^{19}	−2	0	estimated by Glaude *et al.*[54]
15	$PO(OH)_2 + OH = HOPO_2 + H_2O$	2.00×10^{13}	0	0	calculation data
16	$PO(OH)_2 + H = HOPO_2 + H_2$	5.00×10^{12}	0	0	the same
17	$PO(OH)_2 + OH = PO(OH)_3$	1.00×10^{13}	0	0	estimated by Glaude *et al.*[54]
18	$PO(OH)_2 + O = HOPO_2 + OH$	5.00×10^{13}	0	0	the same
19	$P_2O_4 + H_2O = HOPO + HOPO_2$	1.00×10^{11}	0	0	calculation data
20	$P_2O_5 + H_2O = HOPO_2 + HOPO_2$	1.00×10^{11}	0	0	the same
21	$HOPO_2 + O = OH + PO_3$	1.00×10^{13}	0	51664.8	see [f]
22	$HOPO_2 + OH = H_2O + PO_3$	1.20×10^{6}	2	8360	see [g]
23	$HOPO + HO_2 = HOPO_2 + OH$	1.50×10^{14}	0	98648	see [h]
24	$HOPO_2 + HO_2 = H_2O_2 + PO_3$	2.50×10^{12}	0	103078.8	see [i]
25	$HOPO_2 + O_2 = HO_2 + PO_3$	7.00×10^{12}	0	276130.8	see [j]
26	$HOPO_2 + CH_3 = CH_4 + PO_3$	1.50×10^{12}	0	54758	see [k]
27	$PO + OH + M = HOPO + M$ (low pressure) [b]	1.00×10^{21}	−2.09	6646.2	see [a]
28	$PO_2 + H + M = HOPO + M$ (low pressure) [b]	4.87×10^{24}	−2.04	2698.6	see [a, d, l]
29	$HOPO + H = H_2 + PO_2$	1.00×10^{13}	0	45980	calculation data
30	$HOPO + O = OH + PO_2$	1.00×10^{13}	0	0	estimated by Glaude *et al.*[54]
31	$HOPO + O = H + PO_3$	1.00×10^{12}	0	62700	the same
32	$HOPO + HO = PO_2 + H_2O$	1.20×10^{6}	2	−6270	see [d, m]
33	$HOPO + HO_2 = H_2O_2 + PO_2$	2.50×10^{12}	0	97394	estimated by Glaude *et al.*[54]
34	$HOPO + O_2 = HO_2 + PO_2$	7.00×10^{12}	0	189354	see [j]
35	$HOPO + CH_3 = CH_4 + PO_2$	1.50×10^{12}	0	54758	estimated by Glaude *et al.*[54]
36	$PO + O + M = PO_2 + M$ (low pressure) [b]	1.60×10^{25}	−2.63	7189.6	see [a]
37	$PO + OH = H + PO_2$	1.00×10^{13}	0	0	see [n]
38	$PO + HO_2 = PO_2 + OH$	2.10×10^{12}	0	−2090	see [o]
39	$PO + O_2 = PO_2 + O$	1.00×10^{12}	0	0	see [p]
40	$PO + CH_3 = CH_3PO$	1.00×10^{13}	0	0	estimated by Glaude *et al.*[54]
41	$PO_2 + O + M = PO_3 + M$ (low pressure) [b]	1.30×10^{27}	−3.15	7858.4	see [a]
42	$PO_3 + H = PO_2 + OH$	3.16×10^{13}	0	167.2	date from Ref. 62
43	$PO_2 + HO_2 = OH + PO_3$	5.00×10^{11}	0	0	estimated by Glaude *et al.*[54]
44	$PO_2 + O_2 = O + PO_3$	1.00×10^{12}	0	125400	the same
45	$PO_2 + CH_3 = CH_3PO_2$	6.30×10^{14}	−0.60	0	the same [q]
46	$PO_2 + CH_3 = CH_3OPO$	2.10×10^{12}	−0.60	0	the same [r]
47	$PO_2 + CH_3 = CH_3O + PO$	5.00×10^{11}	0	180994	the same
48	$PO_2 + CH_3O = CH_2O + HOPO$	1.00×10^{13}	0	0	"
49	$HOPO + PO_3 = PO_2 + HOPO_2$	5.00×10^{11}	0	0	"
50	$PO_3 + PO = PO_2 + PO_2$	5.00×10^{11}	0	0	"
51	$PO_3 + CH_3 = CH_3OPO_2$	5.00×10^{11}	0	0	"
52	$PO_3 + CH_3 = PO_2 + CH_3O$	5.00×10^{11}	0	63954	"
	$PO_2 + CH_3O = PO_3 + CH_3$	5.00×10^{11}	0	45980	"

Table 4 (continued).

Number of the reaction	Reaction	A	n	E_a /J mol^{-1}	Notes
53	$PO_3 + CH_3O = CH_2O + HOPO_2$	1.00×10^{13}	0	0	estimated by Glaude *et al.*[54]
54	$CH_3 + H = CH_3 + HPO$	1.00×10^{13}	0	25080	the same
55	$CH_3PO + O = CH_3 + PO_2$	1.00×10^{13}	0	0	"
56	$CH_3PO_2 = CH_3PO + O$	1.00×10^{14}	0	555940	"
57	$PO + H + M = HPO + M$ (low pressure) [b]	1.80×10^{22}	−1.95	5559.4	see [a]
58	$HPO + H = H_2 + PO$	2.40×10^{8}	1.50	0	estimated by Glaude *et al.*[54]
59	$HPO + O = OH + PO$	1.70×10^{8}	1.50	0	the same
60	$HPO + O = PO_2 + H$	1.00×10^{13}	0.00	12540	"
61	$HPO + O_2 = PO + HO_2$	7.00×10^{12}	0.00	83600	"
62	$HPO + OH = PO + H_2O$	1.20×10^{6}	2.00	−8360	"
63	$HPO + OH = PO(H)(OH)$	1.40×10^{12}	0	0	estimated by Glaude *et al.*[54]
64	$HOPO + H = H_2O + PO$	3.00×10^{12}	0	34694	see [s]
65	$PO(H)(OH) + H = HOPO + H_2$	5.00×10^{13}	0	0	estimated by Glaude *et al.*[54]
66	$PO(H)(OH) + OH = HOPO + H_2O$	1.00×10^{13}	0	0	the same
67	$PO(H)(OH) + O = HOPO + OH$	5.00×10^{13}	0	0	"
68	$HPO + HO_2 = PO + H_2O_2$	2.00×10^{11}	0	20900	"
69	$HPO + PO_2 = PO + HOPO$	$2.00 \cdot 10^{11}$	0	0	"
70	$HPO + PO_3 = PO + HOPO_2$	2.00×10^{11}	0	0	"
71	$HPO + CH_3 = PO + CH_4$	8.10×10^{5}	1.87	0	"
72	$PO_2 + H + M = HPO_2 + M$ (low pressure) [b]	4.87×10^{21}	−2.04	2696.1	see [d, t]
73	$PO_2 + H + M = HOPO + M$ (low pressure) [b]	4.87×10^{23}	−2.04	2696.1	see [d, u]
74	$HPO_2 = HOPO$	2.35×10^{14}	0	193952	see [v]
75	$HPO_2 + H = H_2 + PO_2$	2.40×10^{8}	1.50	20900	estimated by Glaude *et al.*[54]
76	$HPO_2 + H = PO(H)(OH)$	5.00×10^{12}	0	20900	the same
77	$HPO_2 + O = OH + PO_2$	1.70×10^{8}	1.50	10450	"
78	$HPO_2 + O_2 = PO_2 + HO_2$	7.00×10^{12}	0	143792	"
79	$HPO_2 + OH = H_2O + PO_2$	1.20×10^{6}	2	−8360	"
80	$HPO_2 + OH = H + HOPO_2$	1.00×10^{12}	0	8360	"
81	$HPO_2 + HO_2 = H_2O_2 + PO_2$	2.00×10^{11}	0	41800	"
82	$HPO_2 + CH_3 = CH_4 + PO_2$	8.10×10^{5}	1.87	29260	"
83	$HPO + PO_2 = HPO_2 + PO$	1.00×10^{11}	6.00	0	"
84	$HPO_2 + PO_2 = HOPO + PO_2$	5.00×10^{11}	0	0	"
85	$HPO_2 + PO_3 = HOPO_2 + PO_2$	5.00×10^{11}	0	0	"

[a] The rate constant was taken from Ref. 62 (the expression for the rate constant was converted into the Arrhenius form). [b] The efficiency coefficients for a third body M (H_2O or H_2) are referred to N_2 (the efficiency factor of H_2O is 16, that of H_2 is 2.5). [c] The pre-exponential factor present in the equation for the rate constant for forward reaction was calculated using the pre-exponential factor from the equation for the rate constant for the reverse reaction taking into account partial equilibrium. The activation energy of the forward reaction $CH_3OH + H = CH_3O + H_2$ (elimination of the hydrogen atom) was equal to zero according to calculations. Estimated by Glaude *et al.*[54] [d] The proposed mechanism includes several reactions with identical initial compounds and products but following different channels (for example, elimination and addition reactions). [e] The rate constant was adjusted to the temperature range of 300–2400 K and $P = 1$ atm (see the text). [f] Estimated by Glaude *et al.*[54] The pre-exponential factor of the forward reaction was taken from reaction $CH_3OH + O = CH_3O + OH$.[87] The activation energy of the forward reaction was calculated from the activation energy of reverse reaction taking into account the partial equilibrium. The activation energy of reverse reaction is equal to zero (from the Evans–Polanyi diagramme [88]). [g] According to calculation, the rate constant for reaction (22) is the same as that for $H_2O + OH = H_2O + OH$, estimated by Glaude *et al.*[54] [h] Calculated by analogy with the reaction $CO + HO_2 = CO_2 + OH$ (Ref. 42). Estimated by Glaude *et al.*[54] [i] Calculated by analogy with the reaction $C_2H_5OH + HO_2 = C_2H_5O + H_2O_2$ (Ref. 89). Estimated by Glaude et al.[54] [j] Based on Walker's recommendation for the reactions $RH + O_2 = R + HO_2$ (Ref. 90). Estimated by Glaude *et al.*[54] [k] Calculated by analogy with the reaction $CH_3OH + CH_3 = CH_3O + CH_4$ (Ref. 91). Estimated by Glaude *et al.*[54] [l] Addition of the H atoms to the O atom in PO_2. Rate constant calculated by Twarowski and increased threefold.[65] [m] By analogy with the reaction $ROH + OH = RO + H_2O$ (Ref. 92). The activation energy was taken to be equal to the bond energy H—C (tertiary carbon atom), which corresponds approximately to the H—O bond energy in HOPO. [n] Calculated on the basis of the radical recombination rate. [o] Based on the reaction $NO + HO_2 = NO_2 + OH$ (Ref. 93). Estimated by Glaude *et al.*[54] [p] Calculated on the basis of compact transition state with a zero activation barrier. [q] By analogy with the reaction $CH_3 + NO_2 = CH_3NO_2$ (Ref. 94). [r] By analogy with the reaction $CH_3 + NO_2 = CH_3ONO$ (Ref. 95). [s] The Mackie addition reaction,[55] the pre-exponential factor was decreased. [t] Addition of an H atom to the P atom in PO_2. It is assumed that 1% of all reaction products is HPO_2. [u] Addition of the H atoms to the P atom in PO_2. It is assumed that virtually the whole reaction gives HOPO. The rate constant was taken from Ref. 65. [v] The rate constant was calculated from the BAC MP4 data. The *cis* transition state was used.[96, 97]

these two radicals over the flame zone with and without OPC is an important characteristics. As follows from computation results,[53] DMMP decreases considerably the concentrations of these radicals in both types of flame; the concentration of the H radical decreases faster in the rich flame than in the lean flame. On the basis of foregoing, the authors concluded that there is a difference between the inhibition efficiency of lean and rich flames by OPC [the inhibition efficiency is the difference between the flame propagation speed without an additive (u_0) and with DMMP additive (u) normalised to the flame propagation speed without DMMP: $(u_0-u)/u_0$]. The experimental and computation results were used to plot the dependence of the inhibition efficiency on the equivalence ratio (ϕ). This value proved to be very sensitive to the accuracy of measurement of the combustion rate.‡ The mechanism of flame inhibition by OPC additives developed at the Livermore National Laboratory describes well the dependence of the inhibition efficiency on the equivalence ratio.

According to simulation data,[98] the efficiency of flame propagation inhibition by the addition of DMMP increases monotonically with an increase in the equivalence ratio from 0.8 to 1.3. However, when experimenting with rich and lean flames, Jayaweera *et al.*[53] did not find any significant difference between the DMMP action on these flames, and only calculations did show a slight difference in the inhibition efficiency. To gain an understanding of how OPC inhibit lean and rich flames, the inhibition cycles of these flames were studied in detail.[53] Using PREMIX software,[99] the authors simulated the concentration profiles of OPC involved in the recombination of H and OH radicals in freely propagating propane–air flame with DMMP additive at $P = 1$ atm and calculated the profiles for the formation rates of PO_2 in lean and rich flames (Fig. 17 *a* and *b*, respectively). It follows from the obtained data that the major reaction of PO_2 formation in both types of flames is as follows:

$$HOPO + OH = PO_2 + H_2O. \qquad (11)$$

This path to PO_2 is reasonable for a lean flame characterised by high concentrations of OH radicals but for a rich flame characterised by high concentrations of H radicals, it was more reasonable to assume that reaction (10) would be the major path to PO_2.

However, it was found that reaction (10) makes a minor contribution to the formation of PO_2 due to its high activation energy (11 kcal mol^{-1}) [for comparison, the activation energy of reaction (11) equals 1.5 kcal mol^{-1}]. The major path of PO_2 consumption in both flames is reaction (7). Reactions (7) and (11) form together the catalytic cycle $HOPO \Leftrightarrow PO_2$ in which the H and OH radicals recombine to give H_2O.

The sensitivity coefficients (ξ) of reactions (6)–(11) to the concentrations of H atoms were analysed [53] to determine those having the most pronounced effect on the concentration of hydrogen atoms and to identify the key inhibitor. The sensitivity coefficients of particular reactions to the concentrations of H atoms were determined as derivatives of the mass fractions of H atoms with respect to the pre-exponential factor present in the equation for the rate constant (Fig. 18). A negative sensitivity coefficient means that an increase in the reaction rate results in a decrease in the H atom concentration, *i.e.*, inhibition, while a positive coefficient means that an increase in the reaction rate results in an increase in the H atom concentration. Only reactions involving compounds like H_xPO_y were taken into account. It was noted [53] that the sensitivity coefficient of key reaction (1) to the H atom concentration markedly exceeds in magnitude the sensitivity coefficients of other reactions.

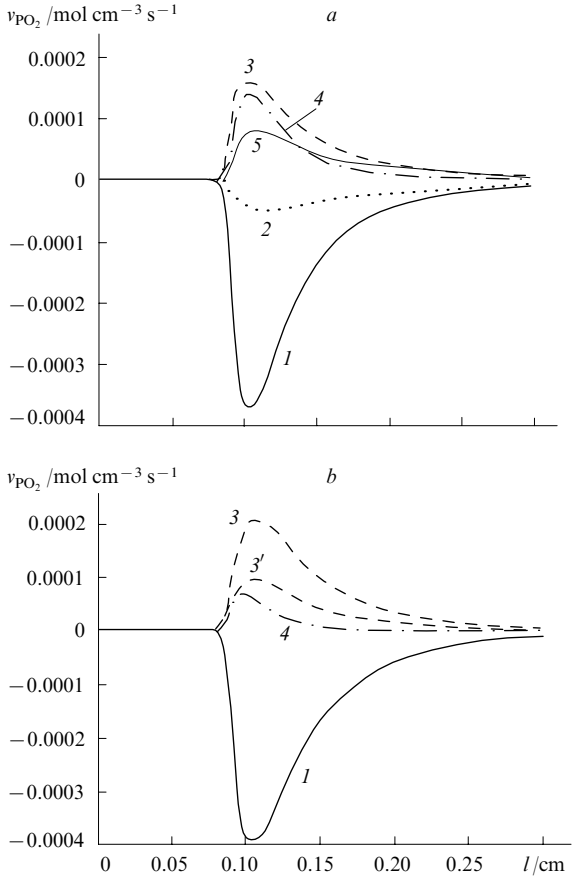


Figure 17. Rates of PO_2 formation and consumption (v_{PO_2}) along reactions (6)–(9) and (11) in lean (*a*) and rich (*b*) flames.[53]
(*1*, *2*) PO_2 consumption by reactions (7) and (6), respectively, (*3*–*5*) PO_2 formation by reactions (11), (8) and (9), respectively (*3*, through H elimination, *3′*, through adduct formation).

It was found [53] that the highest sensitivity of reactions involving H_xPO_y to the H atom concentration in the flame is observed in the post-flame zone. Reaction (7) and, for lean flames, also reaction (9) are most sensitive to the H atom concentration (the rate constant for the latter reaction increases owing to the appearance of a new reaction channel, which was described above).

A curious fact is the increase in the rate of reaction (6) in the lean flame upon an increase in the concentration of H atoms (in the rich flame, the sensitivity of this reaction to the concentration of H atoms is insignificant). The authors believe [53] that the sign of the sensitivity coefficient of reaction (6) to the concentration of H atoms changes owing to the fact that the concentrations of H and OH radicals in the cycle $HOPO \Leftrightarrow PO_2$ decrease faster than in the cycle $HOPO_2 \Leftrightarrow PO_2$. The formation of $HOPO_2$ by reaction (6) results in a decrease in the PO_2 concentration and a decrease in the rate of reaction (7); as a consequence, smaller amounts of H and OH radicals recombine. This suggests that HOPO is a better catalyst than $HOPO_2$. In a lean flame where the $HOPO_2$ concentration is higher than in a rich flame, a lower inhibition efficiency should be expected. The data of calculation of the relative change in the flame propagation speed (see below) also demonstrate that phosphorus inhibits flame less efficiently in lean mixtures than in rich mixtures.

‡ Note that the accuracy of measurements of propagation speeds of rich flames is relatively low. This hampers comparison of the experimental and calculation data.

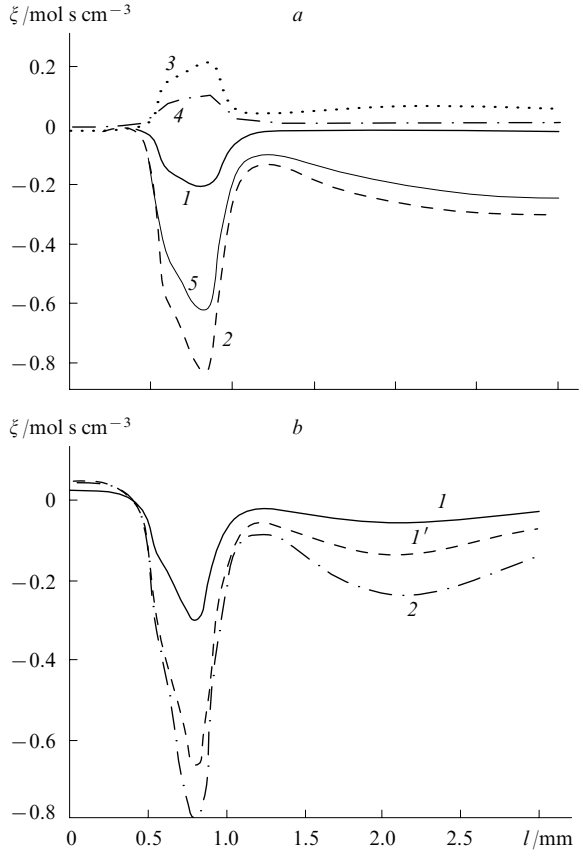


Figure 18. Sensitivity of reactions involving H_xPO_y taking place in lean (*a*) and rich (*b*) flames to H atom concentration:[53] (*1*, *1′*) reactions (11) (*1*, through adduct formation, *1′*, through H atom elimination); (*2*) reactions (7); (*3*) reactions (6); (*4*) reactions (12); (*5*) reactions (9).

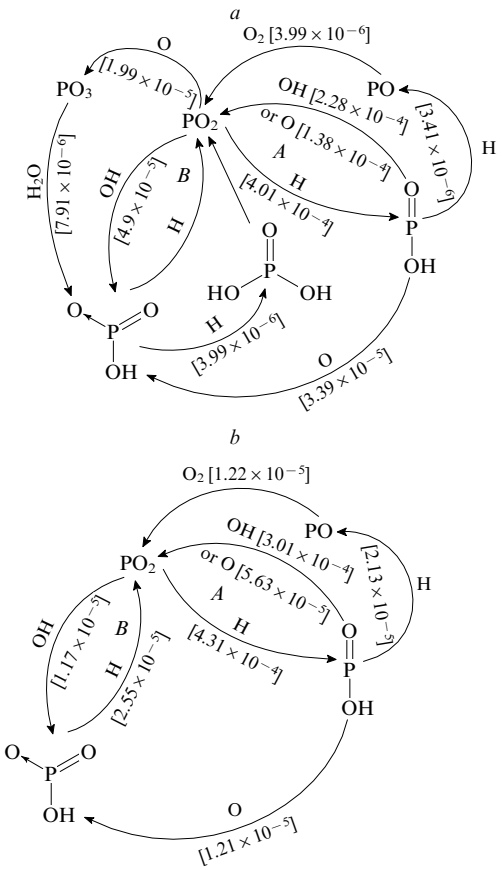


Figure 19. Transformation paths of PO_2 in lean (*a*) and rich (*b*) flames.[53]

The sensitivity of other reactions was interpreted [53] proceeding from the fact that recombination of the H and OH atoms is more efficient in the catalytic cycle $HOPO \Leftrightarrow PO_2$ than in the cycle $HOPO_2 \Leftrightarrow PO_2$. The increase in the rate constants of reactions that direct the reaction stream along the more efficient cycle $HOPO \Leftrightarrow PO_2$ leads to a decrease in the concentrations of the H and OH radicals (flame inhibition), while the increase in the rate constants for reactions that direct the reaction stream through the cycle $HOPO_2 \Leftrightarrow PO_2$ decreases the overall recombination rate of the H and OH radicals and, hence, increases their concentration in the flame.

The reaction

$$HOPO + O = HOPO_2 \qquad (12)$$

that directs the reaction stream along the less efficient cycle accelerates the formation of the H and OH radicals. The same is true for reaction (6). Both reactions have positive sensitivity coefficients to the concentrations of H atoms. Meanwhile, an increase in the rate constant for reaction (9) returns the reaction stream to the more efficient cycle $HOPO \Leftrightarrow PO_2$ and inhibits the formation of the H and OH radicals. The transformation paths of the initial components and final and intermediate products in lean and rich flames are sketched in Figs 19 *a*,*b*, respectively [only reactions with the rates of $> 2 \times 10^{-6}$ mol cm^{-3} s^{-1}, which make the greatest contributions to the formation and consumption of the H and OH radicals (given in brackets §), are given].

§ The reaction rates are given for the distance of 1.07 mm from the burner surface where the PO_2 formation rate is maximum.

It can be seen from Fig. 19 that $HOPO \Leftrightarrow PO_2$ (cycle *A*) and $HOPO_2 \Leftrightarrow PO_2$ (cycle *B*) are the key inhibition cycles. In both cycles, phosphorus compounds act as catalysts of recombination of H and OH radicals to give H_2O. Reaction (12) also takes place being a part of a large cycle. MacDonald *et al.*[100] observed also the recombination of two H atoms with participation of PO_2 and HOPO in diffusion flames. Analysis has shown that recombinations H + OH and H + O predominate over the reaction H + H.

To understand how the two inhibition cycles change with the variation of the equivalence ratio, the extent of oxidation of key phosphorus-containing compounds in lean and rich flames were studied. It could be expected (as was actually shown [52]) that in a lean flame, compounds with a higher oxidation state (for example, $HOPO_2$) would be present in higher concentrations than compounds with lower oxidation state (for example, HOPO). The opposite is true for a rich flame: the HOPO concentration is higher than the $HOPO_2$ concentration. The concentration of HPO is insignificant in both types of flame and has no influence on the reaction rates. As a result of the difference between the HOPO and $HOPO_2$ concentrations, *i.e.*, depending on the equivalence ratio, the directions of the reaction streams change. In both types of flame, the cycle $HOPO \Leftrightarrow PO_2$ is more efficient but in the rich flame where the HOPO concentration is higher than in the lean flame, it is 30% more efficient than the cycle $HOPO_2 \Leftrightarrow PO_2$. In a rich flame, the species PO plays a significant role in the inhibition, while in lean flame, PO_3 is such a species. In the lean flame, the cycle $HOPO_2 \Leftrightarrow PO_2$ is approximately 5 times as significant as in the rich flame owing to the much higher concentration of $HOPO_2$. For this reason, the inhibition path involving $(HO)_2PO$ becomes important.

It should be noted that, although the inhibition efficiencies of the flame involving the catalytic cycles $HOPO_2 \Leftrightarrow PO_2$ and $HOPO \Leftrightarrow PO_2$ are different in lean and rich flames, their total efficiency is comparable in these two cases, *i.e.*, phosphorus 'finds' the most efficient route for flame inhibition. Thus, the ability of phosphorus compound to inhibit flame is unique.

Yet another interesting issue is that the reactions of flame inhibition by phosphorus-containing compounds are most efficient in rather high-temperature regions of the flame at $T > 1600$ K (this corresponds to a distance of 0.9 mm from the burner surface). This is due to the fact that at $T < 1300$ K, the concentrations of all key phosphorus-containing radicals are low (the temperature of 1300 K, which was taken as the reference point, corresponds to consumption of a half of DMMP). The compound $(HO)_2PO$ formed in the beginning of the combustion zone, which is also an inhibitor, is consumed at higher temperature.

The authors [53] pointed to a certain similarity between OPC and the 'ideal' inhibitor described by Rumminger *et al.*,[101] who showed, using a stoichiometric methane–air flame as an example, that at 1 atm an efficient inhibitor starts to operate at $T > 1700$ K and does not lose activity at least up to 2150 K. In the opinion of the researchers cited,[101] the inhibitor that is active at low temperatures is inefficient. This conclusion is based on numerical calculations of the flame propagation speed and structure and on the calculation of the rate of formation and consumption of radicals over the flame zone. Calculations [101] showed that inhibition is most efficient in the case where the maximum chain termination rate in catalytic recombination of H and OH radicals involving the inhibitor coincides with the maximum concentrations of these radicals. Analysis of the model has shown that spatial coincidence of the maximum rates of formation of H atoms according to the quadratic chain branching reaction (1) with the maximum rate of consumption of H atoms in catalytic recombination is the actual criterion.

The studies,[75, 102] which partly confirm the conclusions drawn by Jayaweera *et al.*,[53] are devoted to the structure of methane–oxygen flames with TMP additives stabilised on a flat burner under atmospheric pressure. Figures 20 *a*–*d* show the concentration profiles of the H and OH radicals in lean ($\phi = 0.8$, Fig. 20 *a*,*b*) and rich ($\phi = 1.2$, Fig. 20 *c*,*d*) flames without an additive and with 0.22 vol.% TMP. Note that in the study cited,[102] the concentration profiles of the hydrogen atom in the flame under atmospheric pressure were measured for the first time. It was found that the introduction of the inhibitor results in a sharper decrease in the concentrations of H and OH radicals in a rich flame compared to the lean flame; the most pronounced decrease in the concentrations of H and OH radicals occurs in the zone of chemical reactions rather than in the zone of formation of the final combustion products (which is consistent with the simulation results [53]).

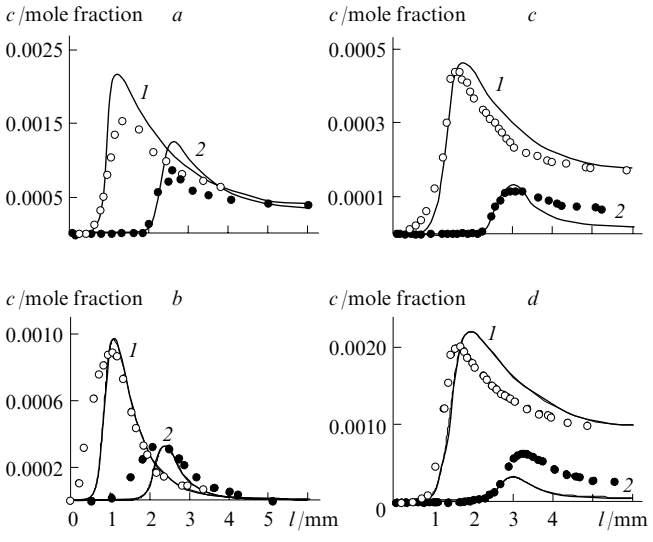


Figure 20. Concentration profiles of H (*b*, *d*) and OH (*a*, *c*) radicals in lean (*a*, *b*) and rich (*c*, *d*) flames without additives (light dots and curves *1*) and with 0.22 vol.% TMP (dark dots and curves *2*).[102]
The dots show experimental values and the lines correspond to simulation results.

It was found [75, 102] that the concentrations of radicals and key phosphorus-containing compounds in the zone of combustion products in inhibited flames under atmospheric pressure are close to equilibrium values. A comparison of experimental data with the results of calculation of the flame structure using the inhibition mechanism [53] shows that in the case of lean flames they are in satisfactory agreement. For rich hydrocarbon flames, the agreement is less satisfactory, which is apparently due to the fact that the inhibition mechanism of rich flames needs to be further developed. This is also indicated by the results of another work [103] dealing with the structure of rich and stoichiometric methane–oxygen flames without additives and with ~0.05 vol.% DMMP at a pressure of 660–670 Torr. The experimental procedure used in the study cited [103] included microprobe sampling of the flame followed by analysis of gaseous products by FT IR spectroscopy. Although the sampling procedure used precluded measurement of the concentrations of labile components, the researchers measured the concentration profiles for formaldehyde, methanol, all C_2 hydrocarbons and the oxides CO and CO_2 in the flame.

It was found that the addition of DMMP into rich flame results in an almost sevenfold increase in the concentration of methanol and a twofold increase in the concentration of acetylene, the ethylene concentration being somewhat decreased. Since the transformation of the CH_3 radical into CH_3OH requires an oxygen atom, while the transformation of CH_3 into C_2 hydrocarbons requires only CH_3, the increase in the CH_3OH concentration may be indicative of the change in the concentration of oxygen atoms in the flame upon the introduction of an inhibitor.

The simulation of the flame structure [103] using two different inhibition mechanisms by OPC additives proposed by Glaude *et al.*[54, 65] showed that neither of these mechanisms predicts correctly the variation of the concentrations of CH_2O, CH_3OH and C_2 hydrocarbons caused by introduction of the inhibitor. The disagreement between the experimental and simulation results indicates that none of the models used in calculations takes into account the most important processes of the chemistry of inhibition of rich flames by OPC. Thus, a mechanism of inhibition of rich flames by OPC additives that would take into account the reactions of phosphorus-containing products with carbon-containing flame components has not been developed so far, which is due to some extent to the lack of understanding of the chemistry of hydrocarbon combustion under conditions of excess fuel and to the lack of the model describing the combustion of rich flames.

b. Propagation speed of flames with organophosphorus additives

The dependence of the speed of free propagation of a 4 : 96 propane–air flame on the concentration of the OPC additive at an initial temperature of 95 °C has been studied.[104] The results of measurements of flame burning velocities with addition of nineteen OPC, including fluorinated OPC, are summarised in Fig. 21. The calculation results for TMP are also presented. The compounds demonstrated similar efficiencies (to within the error of measurements).[104] The OPC used and their boiling points are summarised in Table 5.

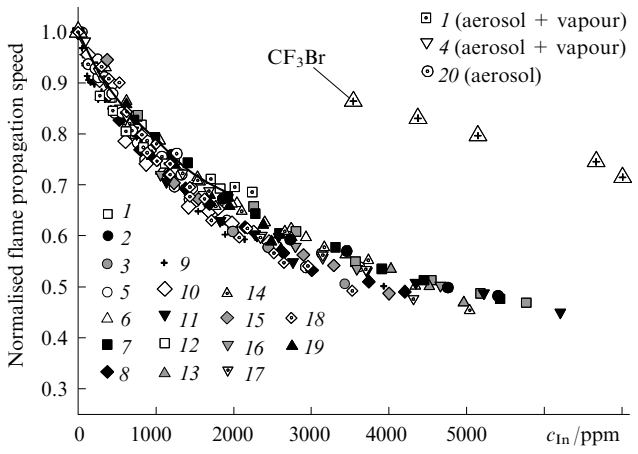


Figure 21. Propagation speed of the $C_3H_8/O_2/N_2$ flame vs. inhibitor concentration (c_{In}).[104]
The inhibitors were a number of OPC (presented in Table 5) and CF_3Br. The dots show experimental values and the lines correspond to simulation results with addition of TMP.

The decrease in the normal propagation speed of the flame upon injection of an inhibitor is due to two factors: chemical (radical decay) and thermal (dilution of the flame with the inhibitor and introduction of additional fuel). The contributions of each factor were identified by analysing the curve for the flame propagation speed *vs.* the limiting concentration of the inhibitor.[105] (This method has been already successfully used to compare the chemical efficiencies of the additives.[106]) After introduction of OPC in low concentrations ($<0.3\%-0.4\%$) into the flame, the decay of radicals in recombination reactions involving these OPC becomes the major factor responsible for the decrease in the combustion rate. Therefore, all compounds show similar efficiencies (see Fig. 21), which almost do not depend on their chemical structure and are determined by the presence of a phosphorus atom in their molecules.

Table 5. Flame suppressants and their boiling points.

Number of the compound	OPC	Boiling point /°C	Pressure / Torr
1	$(CH_3O)_3PO$ (TMP)	180	760
2	$(C_2H_5O)_3PO$	215	760
3	$(CF_3CH_2O)_3PO$	187	760
4	$(HCF_2CF_2CH_2O)_3PO$	90	0.5
5	$(C_3F_7CH_2O)_3PO$	97	2.5
6	$(CH_3O)_2P(O)CH_3$ (DMMP)	181	760
7	$(C_2H_5O)_2P(O)CH_3$	194	760
8	$(CF_3CH_2O)_2P(O)CH_3$	193	760
9	$(C_3F_7CH_2O)_2P(O)CH_3$	92	9
10	$(C_3F_7)_3PO$	144	760
11	$(CH_3O)_3P$	111	760
12	$(C_2H_5O)_2P(O)H$	204	760
13	$(CF_3CH_2O)_2P(O)H$	194	760
14	$(C_2H_5O)_3P$	158	760
15	$(CF_3CH_2O)_3P$	131	760
16	$(HCF_2CF_2CH_2O)_3P$	95	3
17	$(CF_3CH_2O)_2P(O)CF_3$	147	760
18	$(CF_3CH_2O)_2PO(OCH(CF_3)_2)$	83	10
19	$POCl_3$	105	760
20	H_3PO_4 (60% aq. solution)	–	–
21	$(HCF_2CF_2CH_2O)_2P(O)CH_3$	115	6

The effect of TMP (0.06 vol.%) on the propagation speed of methane–air flames at a mixture temperature of 35 °C has been studied as a function of the composition of the mixture (the ϕ value varied from 0.75 to 1.45).[75] The flame propagation speed was measured by measuring the heat flux to the burner[23,24] and calculated in terms of the mechanism of flame inhibition by phosphorus compounds described by Jayaweera *et al.*[53,86] and two mechanisms of methane oxidation, namely, the GRI[46] and the Curran[50,51] mechanisms (Fig. 22).

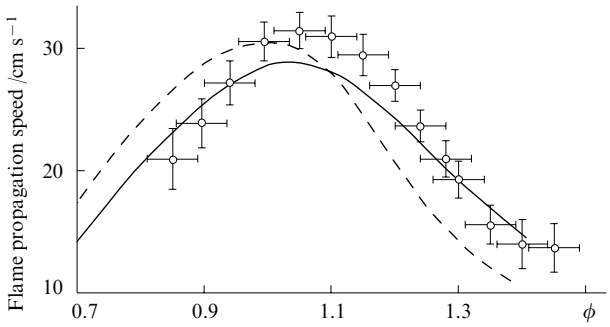


Figure 22. Propagation speed of methane–air flames with 0.06 vol.% TMP *vs.* ϕ.[75]
The dots show experimental values, the continuous line corresponds to simulation results in terms of the GRI mechanism,[46] and the dashed line corresponds to simulation in terms of the Curran mechanism.[50,51]

The calculated flame propagation speeds depended on the selected mechanism of methane oxidation; none of the mechanisms used provided a satisfactory description for the measured dependence of the combustion rate on the equivalence ratio over the whole range (this is one more piece of evidence pointing to imperfection of the proposed multistage kinetic models for hydrocarbon combustion).

Figure 23 shows the efficiency of flame inhibition (E_f) *vs.* ϕ. The value

$$E_f = \frac{u_0 - u}{u_0}$$

was determined from the experimental and simulated data. All curves (both those calculated from experimental data and those obtained by simulation) had a maximum at $\phi = 1.1-1.3$. The calculation data predict an increase in the inhibition efficiency in the range $\phi = 0.7-1.2$, which is attrib-

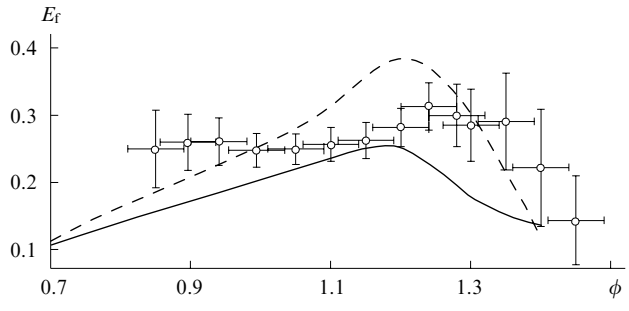


Figure 23. Inhibition efficiency (E_f) *vs.* ϕ.[104]
The dots show experimental values, the continuous line corresponds to simulation results in terms of the GRI mechanism,[46] and the dashed line corresponds to simulation in terms of the Curran mechanism.[50,51]

utable to higher efficiency of the cycle $PO_2 \Leftrightarrow HOPO$ compared to $PO_2 \Leftrightarrow HOPO_2$. The inhibition efficiency calculated from experimental data is almost invariable over this range of ϕ. The decrease in the inhibition efficiency in rich flames was attributed [74] to incomplete destruction of phosphorus-containing products of TMP destruction into active inhibitors, *viz*., phosphorus oxides and phosphorus-containing acids. The results indicate that further studies of the OPC combustion chemistry are required in order to elucidate the inhibition mechanism of flames with a large excess of fuel.

2. Diffusion flames formed at the counterflows of the fuel and the oxidant

Diffusion flames have aroused enhanced interest in recent years. The diffusion flame formed at the counterflows of the fuel and the oxidant is a convenient investigation object for the following reasons. This flame is stabilised in space between the nozzles at a certain distance from them under nearly adiabatic conditions. Although the diffusion flame is two-dimensional, the simulation of its structure can be reduced to a one-dimensional problem, which is implemented in the readily available OPDIFF programme.[35] This allows one to compare experimental data on the flame structure with simulation results and make counterflow flames a convenient investigation object in the OPC combustion chemistry.

Consider the series of papers [36, 37, 107] devoted to the effect of OPC on diffusion flames stabilised on the Potter burner with fuel and oxidant counterflows. Diffusion flames are 'stretched'. An important parameter of such flames is the stretch ratio (a, s^{-1}), which is calculated from the relation

$$a = \frac{2V}{L}\left(1 + \frac{V_f}{V_{ox}}\sqrt{\frac{\rho_f}{\rho_{ox}}}\right),$$

where V is the gas linear velocity, L is the distance between the nozzles, ρ is the density (the subscripts f and ox refer to the fuel and the oxidant, respectively). The stretch ratio is actually inversely proportional to the residence time of the reaction mixture in the flame. This value is also called the velocity gradient (the change in the gas flow velocity in the space between two nozzles).

Typical stretch ratio values for counterflow flames are 100 to 800 s^{-1}. The higher the fuel and oxidant feed rates, the greater the flame stretch ratio. Finally, at a certain stretch ratio (quenching stretch ratio), the flame is quenched. The inhibitor (flame suppressant) decreases the stretch ratio needed to quench the flame; therefore, the efficiency of flame suppressants can be conveniently determined from the dependence of the quenching stretch ratio of a flame on the flame suppressant concentration.

The parameter E_q calculated from the formula

$$E_q = \frac{a_{q0} - a_q}{a_{q0}},$$

where a_{q0} is the quenching stretch ratio for a pure flame, a_q in the quenching stretch ratio for an inhibited flame, has been proposed [100] for comparison of the efficiency of counterflow flame quenching by various inhibitors. The subscript q (quenching) implies that all parameters correspond to the instant of quenching. It was found that DMMP and TMP are 2–4 times more efficient suppressants than CF_3Br.[7, 63, 108, 109] The introduction of a phosphorus-containing compound (1500 ppm) decreases the quenching stretch ratio of the flame by 35%. The injection of the additive into the oxidant flow in a diffusion methane — air flame was found to be 2–4 times more efficient than injection into the fuel flow (in this case, a region with excess fuel is formed on the fuel injection side in the diffusion flames).[109] This is attributable to low inhibition efficiency of rich flames ($\phi > 1.2$) by phosphorus compounds.[75]

The efficiency of quenching of the counterflow $CH_4/O_2 - O_2/N_2$ flame (0.2/0.8 – 0.4/0.6) by fourteen OPC and CF_3Br was studied (Fig. 24, the OPC numbering is the same as in Table 5).[104] The additives were injected into the oxidant flow whose temperature was 100 °C. The plots for the quenching stretch ratio *vs*. the inhibitor concentration were compared with the quenching stretch ratios obtained with one of the most effective inhibitors, *viz*., iron pentacarbonyl $Fe(CO)_5$ (curve *2* in Fig. 24).[110]

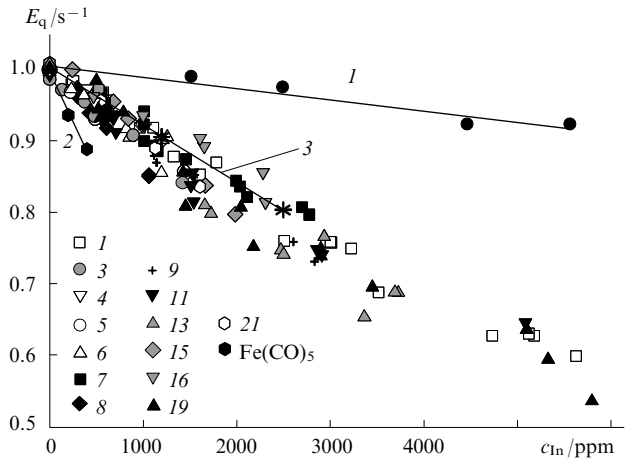


Figure 24. Quenching stretch ratio (E_q) of counterflow flames *vs*. initial concentration of the inhibitor (c_{In}).[104]
Inhibitor: OPC (compound numbering is the same as in Table 5), CF_3Br (curve *1*), $Fe(CO)_5$ (curve *2*); (*3*) calculation results for TMP.

According to the measurement results, at $c_{In} < 0.1$ vol.%, all of the OPC had equal efficiency, which was 7 times higher than that of CF_3Br but 3 times lower than that of iron pentacarbonyl. These results indicate that the efficiency of OPC depends on the concentrations of phosphorus oxides and phosphorus acids and hardly depends on the structure of the initial molecule. The quenching stretch ratios (curve *3* in Fig. 24) for the flames with 0.12 vol.% and 0.25 vol.% TMP (designated by ✱ in Fig. 24) calculated in terms of the mechanism of inhibition by OPC proposed by Korobeinichev *et al*[58, 85] were compared with the experimental data. It was found experimentally that the quenching stretch ratio decreases by 10% and 20% in the presence of 0.12 vol.% and 0.25 vol.% TMP, respectively. The values predicted by numerical simulation are 9.4% and 18.8%. Thus, the results of measurements are in good agreement with the computation data.

The chemical structure of counterflow flames (diffusion or premixed) was studied by laser-induced fluorescence [7, 8, 111, 112] and probe mass spectrometry techniques.[113–115] The molecular-beam mass spectrometry was first applied to probing of a counterflow diffusion flame by Marinov *et al*.[116] The concentration profiles of stable components and phosphorus compounds were obtained and the concentration profile of the OH radical in the flame without additives and with 0.12 vol.% TMP was measured.[113–118]

Analysis of the concentration profiles of phosphorus oxides and phosphorus acids shows that the composition of these compounds in the 'lean' region of the diffusion flame (where excess oxygen is present) is the same as their composition in a lean premixed flame in which $HOPO_2$ predominates.[75, 102] In the 'rich' region of the diffusion flame, the

HOPO is the main phosphorus-containing component, which is typical of rich premixed flames.[75, 102] The numerical calculation of the flame temperature and comparison of the obtained data with the results of measurements have shown that the temperature measurement by a thermocouple arranged on the burner axis gives results that best coincide with the computation results.

The flame structure was also calculated upon simulation in terms of the mechanism of inhibition by OPC.[53, 85] The calculated concentration profiles describe experimental data with a satisfactory accuracy; however, the experimental concentration profiles of compounds in the flame are somewhat broadened compared to calculated profiles, which is due to imperfection of the model used in the OPPDIF programme (the model neglects the edge effects).

3. Air co-flow diffusion flames

The studies of air co-flow diffusion flames were aimed first of all at determining the minimum quenching concentrations of flame suppressants by the cup burner method. Studies of OPC containing no fluorine atoms showed that they are combustible and useless as flame suppressant; therefore, fluorine-substituted OPC were chosen. The MQC values for fluorine-containing organophosphorus inhibitors were measured by the cup burner method independently by Russian [31] and American [119] research groups. In both cases, almost identical cup burners were used, the flame suppressant was supplied through a nebulizer, and the only difference was in the air flow temperature: in one study,[119] the measurements were carried out at 55 °C and in the other study,[31] at 75 °C. In the latter work,[31] five fluorine-containing OPC and CF_3Br were additionally studied (note that organofluorine compounds proved to be less effective than OPC). The measured MQC values are summarised in Table 6. The minimum quenching concentrations are usually expressed as volume fractions or percent, but for practical purposes it is required to know the mass MQC. Analysis of the data presented in Table 6 shows that many fluorine-containing OPC are capable of flame quenching when present in low volume concentrations; however, owing to high molecular masses, their weight consumption exceeds that of less effective CF_3Br. Unfortunately, it was impossible to extinguish the flame with $(CF_3)_3PO$, which has low molecular mass,[119] apparently due to its combustibility.

Table 6. Minimum quenching concentrations of fluorine-substituted OPC and CF_3Br.[31]

Compound	Minimum quenching concentration	
	vol.%	g m^{-3}
$[(CF_3)_2CHO]_2PO(C_2H_5)$	2.0 ± 0.2	366
$[(CF_3)_2CHO]_3P$	2.2 ± 0.2	523
$(CF_3CH_2O)_2PO(CF_3)$	2.3 ± 0.2	322
$(CF_3CH_2O)_3P$	2.6 ± 0.2 (3.1) [a]	381
$(CF_3CH_2O)_2PO[OCH(CF_3)_2]$	no quenching at 3% concentration	–
$(CF_3CH_2O)PO[OCH(CF_3)_2]_2$	burns	–
$(CF_3CH_2O)_2PO(C_2H_5)$	"	–
$[(CF_3)_2CHO]_2PO(CH_3)$	3.0 ± 0.2	530
$[(CF_3)_2CHO]_2PO(CF_3)$	2.0 ± 0.2	400
$(CF_3)_3PO$	no quenching at 5% concentration (see [a])	–
$(CF_3)_2(CH_3O)P$	ignites in air [a]	–
$(CF_3CH_2O)_2P(CF_3)$	3.0 [a]	400
$(CH_3O)PO(CF_3)_2$	4.6 [a]	443
$(CF_3CH_2O)P(CF_3)_2$	1.8 [a]	215
$(CF_3CH_2O)PO(CF_3)_2$	no quenching at 5% concentration (see [a])	–
CF_3Br	4.6	306

[a] Data from Ref. 119.

The results of cup burner experiments give not only the MQC values, but also the dependence of the quenching concentration of one flame suppressant (often an inert diluent, for example, CO_2) on the quenching concentration of the other one, often an active agent. Figure 25 shows the dependences of the quenching concentration of CO_2 on the quenching concentration of fluorine-containing OPC, organofluorine compounds and CF_3Br. It can be seen from the presented data that despite the different MQC values, all phosphorus-containing flame suppressants have similar efficiencies (when present in concentration of $\sim 0.5\%$). Note that the quenching concentration of CO_2 ceases to decrease with an increase in the quenching concentration of some OPC [for example, $(CF_3CH_2O)_2(C_2H_5)PO$], which is indicative of combustibility of these compounds under these conditions (the heat evolved upon their combustion counterbalances the inhibitory effect).

British researchers [120, 121] used an advanced flame ionisation detector (FID) of a chromatograph to study quenching of air co-flow diffusion flames (hydrogen – air and methane – air) by flame suppressants. They tested a large number of OPC. When methane – air flame was used, the MQC values of flame suppressants determined by this and by the cup burner techniques coincided with satisfactory accuracy. The advantage of the FID method [120, 121] is the possibility of using a small amount of a flame suppressant for determining its MQC. Despite the encouraging results and the simple design, the FID method has not yet found extensive use.

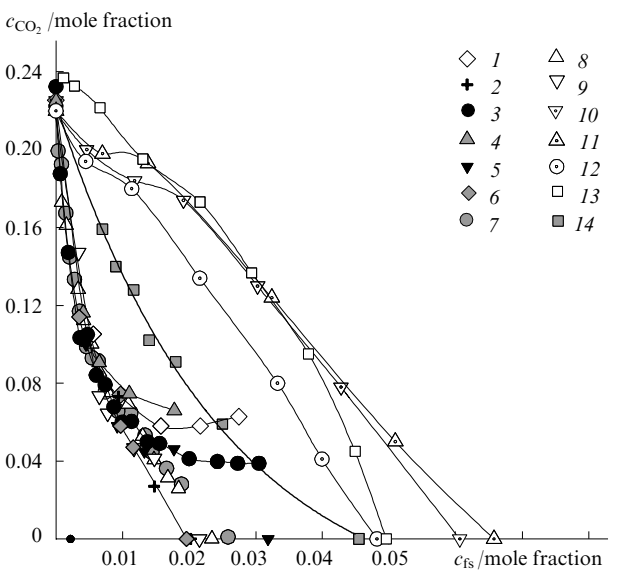


Figure 25. Quenching concentration of CO_2 *vs*. quenching concentration (c_{fs}) of fluorine-substituted OPC (curves *1–9*), organofluorine compounds (curves *10–13*) and CF_3Br (curve *14*).[31]
Compounds: (*1*) $(CF_3CH_2O)_2PO(C_2H_5)$, (*2*) $[(CF_3)_2CHO]_2PO(C_2H_5)$, (*3*) $(CF_3CH_2O)_2PO[OCH(CF_3)_2]$, (*4*) $(CF_3CH_2O)PO[OCH(CF_3)_2]_2$, (*5*) $[(CF_3)_2CHO]_2PO(CH_3)$, (*6*) $[(CF_3)_2CHO]_2PO(CF_3)$, (*7*) $(CF_3CH_2O)_3P$, (*8*) $(CF_3CH_2O)_2PO(CF_3)$, (*9*) $[(CF_3)_2CHO]_3P$, (*10*) $HCF_2CF_2CH_2OCF_2CHFCF_3$, (*11*) $CF_3CF_2CF_2OCHFCF_3$, (*12*) $(CF_3)_2C{=}CFCF_2CF_3$, (*13*) $(CF_3)_2CFCF{=}CFCF_3$, (*14*) CF_3Br.

4. Turbulent flames

The efficiency of quenching turbulent flames by short-term injection of $(CF_3CH_2O)_3P$ and CF_3Br into the air stream was determined [31] on a test bench analogous to that described in

Table 7. Parameters GWP and HGWP calculated for different time ranges characterising the effect of OPC on climatic changes.

Compound	HGWP				GWP			
	20 years	100 years	500 years	∞	20 years	100 years	500 years	∞
$P_3N_3F_6$	0.1	43.5	12.9	4.0	6.9×10^{-3}	2.8×10^{-3}	2.5×10^{-3}	0
$(CF_3CH_2O)_3P$	7.56×10^{-4}	3.1×10^{-4}	2.74×10^{-4}	2.71×10^{-4}	4.8	0.43	0.426	0.426

Ref. 30. A study of the temperature dependence of the MQC of the phosphite $(CF_3CH_2O)_3P$ in the air temperature range of 35 to 86 °C showed [31] that at $T < 60$ °C some of the flame suppressant occurs as an aerosol and some as vapour; therefore MQC is the sum of concentrations. When $T > 60$ °C, MQC corresponds only to the concentration of flame suppressant vapour.

For $T = 75$ °C, the MQC measured for the turbulent flame equals 4 vol.%, which is approximately 1.5 times higher than the concentration measured for the diffusion flame by the cup burner technique. The difference may be related to either the loss of $(CF_3CH_2O)_3P$ during its supply to the flame or to the fact that quenching of the turbulent flame differs appreciably from quenching of the laminar flame. No such difference was observed in determination of the MQC of CF_3Br;[31] however, the coincidence of its MQC values may be accidental.

It was impossible to determine the MQC of trimethyl phosphate,[31] because after the flame quenching, the mixture of TMP vapour with air and combustion products self-ignited.¶ It was found that at an air temperature of 90 °C and a TMP concentration of 8.5 vol.%, no repeated ignition of TMP vapour takes place; however, this quenching concentration can hardly be considered minimum.

VI. Toxicity and environmental impact of organophosphorus compounds

1. Determination of toxicity

In order to evaluate the prospects of using OPC as flame suppressants, the toxicity of a number of OPC was studied. For example, the toxicities of TMP, DMMP, DEMP, tris(2,2,2-trifluoroethyl) phosphate, trimethyl phosphite and tris(2,2,2-trifluoroethyl) phosphite were assessed.[123] The toxicological parameters were measured for laboratory mice upon intragastric administration of the tested compounds in various doses. Dimethyl and diethyl methylphosphonates were dissolved in water prior to the measurements and $(CF_3CH_2O)_3PO$, which is almost insoluble in water, was used as an emulsion in olive oil. Each test series was carried out for 4–8 mice.

The toxicity (LD_{50}) of the OPC upon intragastric administration was relatively low ranging from 0.27 to 10.5 ± 0.09 ml per kg of live weight.[123] DMMP was least toxic, while tris(2,2,2-trifluoroethyl) phosphite was the most toxic. No action of these compounds to skin or mucous membranes was observed.

The toxicity of tris(2,2,2-trifluoroethyl) phosphite vapour upon inhalation was also assessed. The concentration of tris(2,2,2-trifluoroethyl) phosphite vapour at 25 °C is 0.4 vol.% (59 mg litre^{-1}). This concentration was not lethal for mice, which have spent 15 min in a chamber with atmosphere saturated with the phosphite vapour. They all survived for 5 weeks. However, when the temperature in the chamber was raised to 30–35 °C and the OPC concentration increased to 0.68 vol.% (100 mg litre^{-1}), one mice died within 15 min after inhalation of $(CF_3CH_2O)_3P$ vapour and the other four mice died after 2 days. The animal death was due to lung damage. Although the toxicological parameters (LC_{50}) of the tris(2,2,2-trifluoroethyl) phosphite vapour could not be determined, it is obvious that the vapour toxicity is much higher than that of intragastrically administered liquid compound.

2. Environmental impact of organophosphorus compounds

When assessing the impact of various compounds on the environment, two key factors are considered first of all: their impact on the Earth ozone layer and the contribution to the global warming. The impact on the ozone layer is determined by the dimensionless parameter ODP (ozone depletion potential). Trichlorofluoromethane was used as the reference, its ODP being taken to be unity. The efficient flame suppressant CF_3Br (halon 13B1) the production of which was forbidden by the Montreal Convention efficiently depletes the ozone layer, its ODP being 10.

The effect of $(CF_3CH_2O)_3P$ as a representative of OPC on the environment was studied at the laboratory of the Chemical Physics of Atmosphere of the Institute of Energy Problems of Chemical Physics of the RAS.[124] The calculations showed that ODP of this OPC can be considered to be zero. The presence of $(CF_3CH_2O)_3P$ in the atmosphere in a practically infinite amount does not deplete the ozone layer. According to calculation data, the existence time of $(CF_3CH_2O)_3P$ in the atmosphere is 0.019 years.

The contributions of compounds to the global warming (enhancement of the greenhouse effect) are characterised by two dimensionless parameters, the main parameter GWP (Global Warming Potential) and additional parameter HGWP (Halocarbon Global Warming Potential), which is calculated with respect to the GWP of trichlorofluoromethane. The GWP and HGWP parameters are calculated for particular time intervals. The GWP of carbon dioxide for the interval $t = \infty$ is taken to be unity. The GWP and HGWP values for two OPC, *viz.*, phosphazene $P_3N_3F_6$ and tris(2,2,2-trifluoroethyl) phosphite, were calculated.[124] The calculation results are presented in Table 7. The data indicate that these OPC do not possess properties of greenhouse gases and have almost no impact on the Earth climate warming.

* * *

The information summarised in this review shows that considerable progress in the understanding of OPC combustion chemistry has been achieved in the last decade. However, a number of problems still remain unsolved. First of all, this refers to the chemistry of combustion of rich hydrocarbon flames. No data on the combustion chemistry and the mechanism of inhibition of atmospheric hydrogen–oxygen flames, especially rich ones, by organophosphorus compounds are available either, although they are much simpler as regards possible combustion intermediates and final products than hydrocarbon flames.

This review was written with the financial support of the Russian Foundation for Basic Research (Project No. 07-03-11 005-ano).

¶ Previously, it has been shown [122] that TMP vapour burns at elevated temperature.

References

1. R Boyle *Philos. Trans. R. Soc. London* **13** 196 (1680)
2. A Twarowski *Combust. Flame* **94** 91 (1993)
3. *Johnston Atoll Chemical Agent Disposal System. (JACADS). Final Second Supplemental Environmental Impact Statement for the Storage and Ultimate Disposal of the European Chemical Munitions Stockpile, Edgewood, MD, 1990*
4. *Demilitarization and Disposal of U.S. Chemical Warfare Agent and Munitions. Conference on Disarmament*. Ad Hoc Committee on Chemical Weapons. CD/CW/WP. 265 (1989)
5. *World Meteorological Organization Global Ozone Research and Monitoring Project. Scientific Assessment of Stratospheric Ozone, Geneva, 1989* Vol. 1, Report 20
6. J W Hastie, D W Bonnell *Molecular Chemistry of Inhibited Combustion Systems* National Bureau of Standards, NBSIR, 80-2169, 1980
7. M A MacDonald, T M Jayaweera, E M Fisher, F C Gouldin *Combust. Flame* **116** 166 (1999)
8. J E Siow, N M Laurendeau *Combust. Flame* **136** 16 (2004)
9. R M Fristrom, A A Vestenberg *Struktura Plameni* (The Structure of Flame) (Moscow: Metallurgiya, 1969)
10. R M Fristrom, C Grunfelder, S Favin *J. Phys. Chem.* **64** 1386 (1960)
11. O P Korobeinichev, A G Tereshchenko, I D Emel'yanov, L V Kuibida, R A Mavliev, K P Kutsenogii, A L Rudnitskii, S Yu Fedorov, N E Ermolin, V M Fomin *Obosnovanie Metoda Mass-spektrometricheskogo Zondirovaniya Plamen Kondensirovannykh Sistem s Uzkimi Zonami Goreniya* (Substantiation of the Method of Mass-spectrometric Probe for Flames of Condensed Systems with Narrow Combustion Zones) (Novosibirsk: Siberian Branch, Academy of Sciences of the USSR, 1985) Preprint No. 14
12. J H Werner, T A Cool *Chem. Phys. Lett.* **275** 278 (1997)
13. J H Werner, T A Cool *Combust. Flame* **117** 78 (1999)
14. O P Korobeinichev, S B Ilyin, V V Mokrushin, A G Shmakov *Combust. Sci. Technol.* **116** 51 (1996)
15. O P Korobeinichev, V M Shvartsberg, A A Chernov, V V Mokrushin *Proc. Combust. Institute* **26** 1035 (1996)
16. P A Skovorodko, A G Tereshchenko, O P Korobeinichev, D A Knyazkov, A G Shmakov *Khim. Fiz.* **25** 23 (2006) [a]
17. P A Skovorodko, A G Tereshchenko, O P Korobeinichev, D A Knyazkov, A G Shmakov *Khim. Fiz.* **25** 33 (2006) [a]
18. K A Burton, H D Ladouceur, J W Fleming *Combust. Sci. Technol.* **81** 141 (1992)
19. W E Kaskan *Proc. Combust. Institute* **6** 134 (1957)
20. A N Hayhurst, D B Kittelson *Combust. Flame* **28** 301 (1977)
21. O P Korobeinichev, V M Shvartsberg, T A Bolshova, A G Shmakov, D A Knyazkov *Fiz. Goren. Vzryva* **38** (2) 3 (2002) [b]
22. G T Linteris, L Truett *Combust. Flame* **105** 15 (1996)
23. L P H de Goey, A van Maaren, R M Quax *Combust. Sci. Technol.* **92** 1 (1993)
24. A van Maaren, D S Thung, L P H de Goey *Combust. Sci. Technol.* **96** 327 (1994)
25. B Lewiss, G von Elbe *Combustion, Flames and Explosions of Gases* (New York: Academic Press, 1961)
26. *NFPA 2001: Standard on 'Clean Agents Fire Extinguishing Systems', USA, 1994*
27. J D Mather, R E Tapscott, T A Moore *Proceedings of Halon Options Technical Working Conference 1998* CD-ROM NIST SP 948-3, National Institute of Standards and Technology, Gaithersburg, MD, 2005
28. A N Baratov, N P Kopylov, E V Timofeev *Proceedings of Halon Options Technical Working Conference, 2002* CD-ROM NIST SP 948-3, National Institute of Standards and Technology, Gaithersburg, MD, 2005
29. A N Baratov, S G Tsarichenko, A F Zhevlakov, E V Timofeev, R A Yajliyan *Proceedings of the Fourth Asia-Pacific Symposium on Fire Science and Technology, Tokyo, 2000* p. 351
30. W Grosshandler, A Hamins, K McGrattan, C Presser *Transient Application, Recirculating Pool Fire, Agent Effectiveness Screen, Final Report* NGP Project 3A/2/890, National Institute of Standards and Technology, Gaithersburg, MD, 2001
31. A G Shmakov, O P Korobeinichev, V M Shvartsberg, S A Yakimov, D A Knyazkov, V F Komarov, G V Sakovich *Fiz. Goren. Vzryva* **42** (6) 64 (2006) [b]
32. R J Kee, J F Grcar, M D Smooke, J A Miller *Sandia National Laboratories Report, 1990* SAND85-8240
33. R J Kee, F M Rupley, J A Miller *CHEMKIN-II: A Fortran Chemical Kinetics Package for the Analysis of Gas Phase Chemical Kinetics. Sandia National Laboratories Report* New Mexico, CA, 1989, SAND89-8009B
34. C M Lund *HCT — A General Computer Program for Calculating Time-Dependent Phenomena Involving One-Dimensional Hydrodynamics, Transport, and Detailed Chemical Kinetics* Lawrence Livermore National Laboratory, Livermore, CA, 1978, Report UCRL-52504
35. A E Lutz, R J Kee, J F Grcar, F M Rupley *Chemkin Collection, Unlimited Release* Sandia National Laboratories, Livermore, CA, 1997
36. A E Potter, J N Butler *Int. ARS J.* 50 (1959)
37. A E Potter, S Heimel, J N Butler *Proc. Combust. Institute* **9** 1027 (1962)
38. J Warnatz *Combustion Chemistry* (Ed. W C Gardiner) (New York: Springer, 1984)
39. G Dixon-Lewis *Arch. Combust.* **4** 279 (1984)
40. J A Miller, M D Smoke, R M Green, R J Kee *Combust. Sci. Technol.* **34** 149 (1983)
41. G Dixon-Lewis, M M Sutton, A Willams *Proc. R. Soc. London, Ser. A* **317** 227 (1970)
42. W Tsang, J Hampson *J. Phys. Chem. Ref. Data* **15** 1087 (1986)
43. R A Yetter, F L Dryer, H Rabitz *Combust. Sci. Technol.* **79** 97 (1991)
44. D L Baulch, D D Drysdale, D G Horne *Evaluated Kinetic Data for High Temperature Reactions. Homogeneous Gas Phase Reactions of the H_2-O_2 System* (London: Butterworths, 1976) Vol. 1
45. M Ó Connaire, H J Curran, J M Simmie, W J Pitz, C K Westbrook *Int. J. Chem. Kinet.* **36** 603 (2004)
46. G P Smith, D M Golden, M Frenklach, N W Moriarty, B Eiteneer, M Goldenberg, C T Bowman, R K Hanson, S Song, W C Gardiner Jr, V V Lissianski, Z Qin *GRI Mech 3.0* 1999; http://www.me.berkeley.edu/gri_mech
47. A Konnov *Detailed Reaction Mechanism for Small Hydrocarbons Combustion* Release 0.5, http://homepages.vub.ac.be/∼akonnov
48. A van Maaren, L P H de Goey *Combust. Sci. Technol.* **102** 309 (1994)
49. C M Vagelopoulos, F N Egolfopoulos, C K Law *Proc. Combust. Institute* **25** 1341 (1994)
50. M Ó Connaire, H J Curran, J M Simmie *Proceedings of the European Combustion Meeting, Orléans, France, 2003*
51. H J Curran, T M Jayaweera, W J Pitz, C K Westbrook *Western States Section of the Combustion Institute, Davis, CA, 2004* Paper 04S-58
52. O P Korobeinichev, V M Shvartsberg, A G Shmakov, T A Bolshova, T M Jayaweera, C F Melius, W J Pitz, C K Westbrook, H Curran *Proc. Combust. Institute* **30** 2353 (2005)
53. T M Jayaweera, C F Melius, W J Pitz, C K Westbrook, O P Korobeinichev, V M Shvartsberg, A G Shmakov, I V Rybitskaya, H J Curran *Combust. Flame* **140** 103 (2005)
54. P A Glaude, H J Curran, J W Pitz, C K Westbrook *Proc. Combust. Institute* **28** 1749 (2000)
55. J C Mackie, G B Bacskay, N L Haworth *J. Phys. Chem. A* **106** 10825 (2002)
56. C W Bauschlicher *J. Phys. Chem. A* **103** 11126 (1999)
57. O P Korobeinichev, A A Chernov, V M Shvartsberg *Prepr. Pap. Am. Chem. Soc., Div. Fuel Chem.* **39** (1) 193 (1994)
58. O P Korobeinichev, S B Ilyin, T A Bolshova, V M Shvartsberg, A A Chernov *Combust. Flame* **121** 593 (2000)
59. S B Il'in, Candidate Thesis in Physical and Mathematical Sciences, Institute of Chemical Kinetics and Combustion, Siberian Branch of the Russian Academy of Sciences, Novosibirsk, 1998
60. E R Wils *Fresenius' J. Anal. Chem.* **338** 22 (1990)
61. A Twarowski *Combust. Flame* **94** 341 (1993)
62. A Twarowski *Combust. Flame* **102** 41 (1995)
63. A Twarowski *Combust. Flame* **105** 407 (1996)

64. O P Korobeinichev, V M Shvartsberg, A A Chernov *Combust. Flame* **118** 727 (1999)
65. R T Wainner, K L McNesby, A W Daniel, A W Miziolek, V I Babushok *Proceedings of Halon Options Technical Working Conference, 2000* CD-ROM NIST SP 948-3, National Institute of Standards and Technology, Gaithersburg, MD, 2005
66. O P Korobeinichev, S B Ilyin, V M Shvartsberg, A A Chernov *Combust. Flame* **118** 718 (1999)
67. V M Shvartsberg, Candidate Thesis in Chemical Sciences, Institute of Chemical Kinetics and Combustion, Siberian Branch of the Russian Academy of Sciences, Novosibirsk, 2000
68. O P Korobeinichev, V M Shvartsberg, S B Il'in *Fiz. Goren. Vzryva* **33** (3) 32 (1997) [b]
69. O P Korobeinichev, T A Bolshova, V M Shvartsberg, A A Chernov *Combust. Flame* **125** 744 (2001)
70. R Atkinson *J. Chem. Phys. Ref. Data (Monograph I)* 201 (1989)
71. O P Korobeinichev, A A Chernov, T A Bolshova *Combust. Flame* **123** 412 (2000)
72. E J P Zegers, E M Fisher *Combust. Flame* **115** 230 (1998)
73. P A Glaude, C F Melius, W J Pitz, C K Westbrook *Proc. Combust. Institute* **29** 2469 (2002)
74. O P Korobeinichev, V M Shvartsberg, S B Il'in, A A Chernov, T A Bolshova *Fiz. Goren. Vzryva* **35** (3) 29 (1999) [b]
75. O P Korobeinichev, V M Shvartsberg, A G Shmakov, D A Knyazkov, I V Rybitskaya *Proc. Combust. Institute* **31** 2741 (2007)
76. O P Korobeinichev, A A Chernov, L N Krasnoperov *Proceedings of International CWA Destruction Symposium, Munster, Germany, 1998* p. 225
77. O P Korobeinichev, A A Chernov, V V Sokolov, L N Krasnoperov *Int. J. Chem. Kinet.* **34** 331 (2002)
78. O P Korobeinichev, A A Chernov, V V Sokolov, L N Krasnoperov *Khim. Fiz.* **21** (12) 27 (2002) [a]
79. T A Bolshova, Candidate Thesis in Physical and Mathematical Sciences, Institute of Chemical Kinetics and Combustion, Siberian Branch of the Russian Academy of Sciences, Novosibirsk, 2006
80. V S Babkin, A V V'yun *Fiz. Goren. Vzryva* **17** (5) 8 (1981) [b]
81. T A Bolshova, O P Korobeinichev *Fiz. Goren. Vzryva* **42** (5) 3 (2006) [b]
82. M R Zachariah, O I Smith *Combust. Flame* **69** 125 (1987)
83. V N Strokin, V M Khailov *Fiz. Goren. Vzryva* **10** (2) 230 (1974) [b]
84. J W Hastie *Int. J. Mass Spectrom. Ion Processes* **16** 89 (1975)
85. O P Korobeinichev, A L Mamaev, V V Sokolov, T A Bolshova; V M Shvartsberg, L Zakharov, I Yu Kudryavtsev *Proceedings Halon Options Technical Working Conference, 2001* CD-ROM NIST SP 948-3, National Institute of Standards and Technology, Gaithersburg, MD, 2005
86. http://www kinetics nsc ru/labor/kcp_en/opc_mech html
87. J Warnatz *Gas-Phase Combustion Chemistry* (Ed. W C Gardiner) (New York: Springer, 2000)
88. M G Evans, M Polanyi *Trans. Faraday Soc.* **34** 11 (1938)
89. N Marinov *Int. J. Chem. Kinet.* **31** 183 (1999)
90. T Ingham, R W Walker, R E Woolford *Proc. Combust. Institute* **25** 767 (1994)
91. W Tsang *J. Phys. Chem. Ref. Data* **16** 471 (1987)
92. R Atkinson *Int. J. Chem. Kinet.* **18** 555 (1986)
93. W B DeMore, S P Sander, D M Golden, R F Hampson, M J Kurylo, C J Howard, A R Ravishankara, C E Kolb, M J Molina *Chemical Kinetics and Photochemical Data for Use in Stratospheric Modeling (Evaluation Number 12), Jet Propulsion Laboratory, California Institute of Technology, Pasadena, CA, 1997* Publication 97-4
94. K Glaenzer, J Troe *Ber. Bunsen-Ges. Phys. Chem.* **78** 182 (1974)
95. C Canosa, R-D Penzhorn, C von Sonntag *Ber. Bunsen-Ges. Phys. Chem.* **83** 217 (1979)
96. C F Melius M D Allendorf *J. Phys. Chem. A* **104** 2168 (2000)
97. C F Melius *Chemistry and Physics of Energetic Materials* (Ed. S N Bulusu) (Dordrecht: Kluwer Academic, 1990) p. 21
98. T M Jayaweera, C F Melius, W J Pitz, C K Westbrook, O P Korobeinichev, V M Shvartsberg, A G Shmakov, I V Pybitskaya, H Curran *Western States Section of the Combustion Institute, Davis, CA, 2004* Paper 042-43
99. R J Kee, F M Rupley, J A Miller, M E Coltrin, J F Grcar, E Meeks, H K Moffat, A E Lutz, G Dixon-Lewis, M D Smooke, J Warnatz, G H Evans, R S Larson, R E Mitchell, L R Petzold, W C Reynolds, M Caracotsios, W E Stewart, P Glarborg, C Wang, O Adigun, W G Houf, C P Chou, S F Miller *Chemkin Collection. Release 3.7.1, Reaction Design, San Diego, CA, 2003*
100. M A MacDonald, F C Gouldin, E M Fisher *Combust. Flame* **124** 668 (2001)
101. M D Rumminger, V I Babushok, G T Linteris *Proc. Combust. Institute* **29** 329 (2002)
102. D A Knyazkov, V M Shvartsberg, A G Shmakov, O P Korobeinichev *Fiz. Goren. Vzryva* **43** (2) 23 (2007) [b]
103. M F M Nogueira, E M Fisher *Combust. Flame* **132** 352 (2003)
104. A G Shmakov, O P Korobeinichev, V M Shvartsberg, D A Knyazkov, T A Bolshova, I V Rybitskaya *Proc. Combust. Institute* **30** 2345 (2005)
105. V V Zamashchikov, V A Bunev *Fiz. Goren. Vzryva* **37** (1) 15 (2001) [b]
106. V V Zamashchikov, V A Bunev *Fiz. Goren. Vzryva* **38** (5) 3 (2002) [b]
107. D A Knyazkov, Candidate Thesis in Physical and Mathematical Sciences, Institute of Chemical Kinetics and Combustion, Siberian Branch of the Russian Academy of Sciences, Novosibirsk, 2006
108. M A MacDonald, T M Jayaweera, E M Fisher, F C Gouldin *Technical Meeting 'Central States Section of The Combustion Institute', Point Clear, AL, 1997*
109. M A MacDonald, T M Jayaweera, E M Fisher, F C Gouldin *Proc. Combust. Institute* **27** 2749 (1998)
110. D Reinelt, G T Linteris *Proc. Combust. Institute* **26** 1421 (1996)
111. R R Skaggs, R G Daniel, A W Miziolek, K L McNesby *Proceedings of the First Joint Meeting of the US Sections of the Combustion Institute, Washington, DC, 1999* p. 575
112. D D Thomsen, N M Laurendeau *Combust. Flame* **124** 350 (2001)
113. S C Li, F A Williams *Proc. Combust. Institute* **28** 1031 (2000)
114. M M Y Waly, F A Williams *Proc. Combust. Institute* **28** 2005 (2000)
115. R Seiser, L Truett, D Trees, K Seshadri *Proc. Combust. Institute* **27** 649 (1998)
116. N M Marinov, W J Pitz, C K Westbrook, A E Lutz, A M Vincitore, S M Senkan *Proc. Combust. Institute* **27** 605 (1998)
117. D A Knyazkov, O P Korobeinichev, A G Shmakov *Fiz. Goren. Vzryva* **42** (4) 26 (2006) [b]
118. D A Knyazkov, A G Shmakov, O P Korobeinichev *Proceedings of the 5th International Seminar on Flame Structure, Novosibirsk, 2005* (Ed. O P Korobeinichev) Paper OP-03 (CD)
119. J D Mather, R E Tapscott, J M Shreeve, R P Singh *Proceedings of Halon Options Technical Working Conferences, 2003* CD-ROM NIST SP 984-4, National Institute of Standards and Technology, Gaithersburg, MD, 2006
120. J Riches, L Knutsen, E Morrey, K Grant *Proceedings of Halon Options Technical Working Conferences, 2000* CD-ROM NIST SP 984-4, National Institute of Standards and Technology Gaithersburg, MD, 2006
121. L Knutsen, E Morrey, J Riches *Proceedings of Halon Options Technical Working Conferences, 2002* CD-ROM NIST SP 984-4, National Institute of Standards and Technology, Gaithersburg, MD, 2006
122. O P Korobeinichev, A G Shmakov, V M Shvartsberg, D A Knyazkov, K P Kutsenogii, V I Makarov, Y M Samsonov, E E Nifantiev, I Yu Kudryavtsev, E I Goryunov, V P Nikolin, B I Kaledin *Proceedings of Halon Options Technical Working Conferences, 2003* CD-ROM NIST SP 984-4, National Institute of Standards and Technology, Gaithersburg, MD, 2006

123. O P Korobeinichev, A G Shmakov, A A Chernov, V M Shvartsberg, I V Rybitskaya, V I Makarov, E E Nifantev, I Y Kudryavtsev, E I Goryunov, V P Nikolin *Proceedings of Halon Options Technical Working Conferences, 2004* CD-ROM NIST SP 984-4, National Institute of Standards and Technology Gaithersburg, MD, 2006
124. A G Shmakov, O P Korobeinichev, D A Knyazkov, V M Shvartsberg, S A Yakimov, A N Baratov, S N Kopylov, D B Zhiganov, I K Larin *Proceedings of Halon Options Technical Working Conferences, 2006* CD-ROM NIST SP 984-4, National Institute of Standards and Technology Gaithersburg, MD, 2006

[a] — *Chem. Phys. Rep. (Engl. Transl.)*
[b] — *Combust. Explos. Shock Waves (Engl. Transl.)*